



저작자표시-비영리-변경금지 2.0 대한민국

이용자는 아래의 조건을 따르는 경우에 한하여 자유롭게

- 이 저작물을 복제, 배포, 전송, 전시, 공연 및 방송할 수 있습니다.

다음과 같은 조건을 따라야 합니다:



저작자표시. 귀하는 원저작자를 표시하여야 합니다.



비영리. 귀하는 이 저작물을 영리 목적으로 이용할 수 없습니다.



변경금지. 귀하는 이 저작물을 개작, 변형 또는 가공할 수 없습니다.

- 귀하는, 이 저작물의 재이용이나 배포의 경우, 이 저작물에 적용된 이용허락조건을 명확하게 나타내어야 합니다.
- 저작권자로부터 별도의 허가를 받으면 이러한 조건들은 적용되지 않습니다.

저작권법에 따른 이용자의 권리는 위의 내용에 의하여 영향을 받지 않습니다.

이것은 [이용허락규약\(Legal Code\)](#)을 이해하기 쉽게 요약한 것입니다.

[Disclaimer](#)

Thesis for the Degree of Master of Science

Future prediction of 1 km precipitation/temperature
and regional analysis of extreme changes according to
RCP scenarios in Korean Peninsula

by

Hyung-Jeon Kang

Department of Environmental Atmospheric Sciences

The Graduate School

Pukyong National University

February 2017

Future prediction of 1 km precipitation/temperature and
regional analysis of extreme changes according to RCP
scenarios in Korean Peninsula

(RCP 시나리오에 따른 한반도의 지역별 1km 상세
미래 강우/기온 전망 및 극한 사상 변화 분석)

Advisor: Prof. Jai-Ho Oh

by

Hyung-Jeon Kang

A thesis submitted in partial fulfillment of the requirements
for the degree of

Master of Science

in Department of Environmental Atmospheric Science, The Graduate School,
Pukyong National University

February 2017

Future prediction of 1 km precipitation/temperature
and regional analysis of extreme changes according
to RCP scenarios in Korean Peninsula

A dissertation
by
Hyung-Jeon Kang

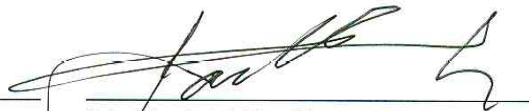
Approved by:



(Chairman) Jae-Jin Kim



(Member) Won-Sik Choi



(Member) Jai-Ho Oh

February, 2017

Contents

List of Figures	iii
List of Tables	vi
Abstract	viii
I. Introduction	1
II. Models, Data and Methodology	7
1. Model description	7
1.1. Quantitative Precipitation Model(QPM)	7
1.2. Quantitative Temperature Model(QTM)	10
2. Data	11
3. Methodology	21
3.1. Restoration of precipitation / temperature on the ungauged site	21
3.2. Observation-based future climate prediction over Korean Peninsula	22
III. Verification	24
1. Verification of restored precipitation / temperature	24
1.1. Verification of restored precipitation data	28
1.2. Verification of restored temperature data	34
2. Evaluation of simulation	39
IV. Results	41
1. Prediction of detailed Future Climate over Korean Peninsula	41
1.1. Prediction of future precipitation change	43
1.2. Prediction of future temperature change	49
2. Changes of extreme events	53

2.1. Changes of extreme events related to precipitation	53
2.2. Changes of extreme events related to temperature	57
V. Conclusion and Summary	61
VI. Reference	63



List of Figures

Fig. 1 DEM data to consider detailed topographic effect(units : m)	6
Fig. 2 Spatial distribution of AWS / ASOS observation (KMA) points (in 2014)	12
Fig. 3 Increase trend of AWS / ASOS observation (KMA) points (2000-2014)	13
Fig. 4 Verification points of each dataset for the best dataset selection	16
Fig. 5 Selected verification points for the verification of restored data	25
Fig. 6 Model Bias of seasonal precipitation between the restored data and produced data from GME model	40
Fig. 7 Model Bias of seasonal temperature between the restored data and produced data from GME model	40
Fig. 8 Selected regions for detailed analysis of the future climate changes over Korean Peninsula	42
Fig. 9 Graph of regional detailed precipitation changes (decadal-average) based on the RCP 8.5 scenario over Korean Peninsula	44
Fig. 10 Graph of regional detailed precipitation changes (decadal-average) based on the RCP 4.5 scenario over Korean Peninsula	44

Fig. 11 Graph of detailed precipitation changes (monthly-average) based on the RCP 8.5 scenario over Seoul regions	46
Fig. 12 Graph of detailed precipitation changes (monthly-average) based on the RCP 4.5 scenario over Seoul regions	46
Fig. 13 Graph of detailed precipitation changes (monthly-average) based on the RCP 8.5 scenario over Busan regions	47
Fig. 14 Graph of detailed precipitation changes (monthly-average) based on the RCP 4.5 scenario over Busan regions	47
Fig. 15 Graph of detailed precipitation changes (monthly-average) based on the RCP 8.5 scenario over North Korea regions	48
Fig. 16 Graph of detailed precipitation changes (monthly-average) based on the RCP 4.5 scenario over North Korea regions	48
Fig. 17 Graph of regional detailed temperature changes (decadal-average) based on the RCP 8.5 scenario over Korean Peninsula	50
Fig. 18 Graph of regional detailed temperature changes (decadal-average) based on the RCP 4.5 scenario over Korean Peninsula	50
Fig. 19 Graph of regional detailed temperature changes (monthly-average) based on the RCP 8.5 scenario over Korean Peninsula	52
Fig. 20 Graph of regional detailed temperature changes (monthly-average) based on the RCP 4.5 scenario over Korean Peninsula	52

Fig. 21 Detailed regional heavy-rainfall prediction for the far-future climate based on the RCP 8.5 scenario over Korean Peninsula	55
Fig. 22 Detailed regional heavy-rainfall prediction for the far-future climate based on the RCP 4.5 scenario over Korean Peninsula	55
Fig. 23 Detailed regional precipitation intensity prediction for the far-future climate based on the RCP 8.5 scenario over Korean Peninsula	56
Fig. 24 Detailed regional precipitation intensity prediction for the far-future climate based on the RCP 4.5 scenario over Korean Peninsula	56
Fig. 25 Detailed regional heat wave prediction for the far-future climate based on the RCP 8.5 scenario over Korean Peninsula	59
Fig. 26 Detailed regional heat wave prediction for the far-future climate based on the RCP 4.5 scenario over Korean Peninsula	59
Fig. 27 Detailed regional tropical night prediction for the far-future climate based on the RCP 8.5 scenario over Korean Peninsula	60
Fig. 28 Detailed regional tropical night prediction for the far-future climate based on the RCP 4.5 scenario over Korean Peninsula	60

List of Tables

Table 1 List of available datasets	15
Table 2 Precipitation cases for selecting best datasets	17
Table 3 Results of correlation analysis (Case 1)	19
Table 4 Results of correlation analysis (Case 2)	19
Table 5 Results of correlation analysis (Case 3)	20
Table 6 Results of correlation analysis (Case 4)	20
Table 7 Location (degrees) information for AWS / ASOS stations matching with QPM / QTM model grid points	26
Table 8 Location (degrees) information for GTS stations matching with QPM / QTM model grid points	27
Table 9 2×2 Rain contingency table	28
Table 10 List of selected cases for verification of restored precipitation	30
Table 11 Results of Qualitative verification of restored precipitation over South Korea	31
Table 12 Results of Quantitative verification of restored precipitation over South Korea	32
Table 13 Results of Qualitative verification of restored precipitation over North Korea	33
Table 14 Results of Quantitative verification of restored precipitation over North Korea	33
Table 15 List of selected cases for restored temperature verification	34

Table 16 Results of quantitative verification of restored temperature by cases (Unapplied : Gridded temperature lapse rate unapplied, Applied : Gridded temperature lapse rate applied) 35

Table 17 Results of quantitative verification of restored temperature by verification points 37

Table 18 Results of monthly quantitative verification of restored temperature 38



RCP 시나리오에 따른 한반도의 지역별 1km 상세 미래 강우/기온 전망 및 극한 사상 변화 분석

강형전

부경대학교 대학원 환경대기과학과

요약

본 연구에서는 RCP 시나리오에 따른 40 km 해상도의 전지구 기후모델 GME 자료를 기반으로 정량적 강우 진단 모델 (QPM) / 정량적 기온 진단 모델 (QTM)을 이용하여 통계적 다운스케일링 모델로는 표현되지 않는 물리과정을 고려한 한반도 전체 지역에 대한 1 km 상세 미래 강우/기온을 전망하였다.

관측 자료를 기반으로 한 미래기후 전망 자료를 생산하기 위하여 현재 기후(2000-2014년) 동안의 관측 자료를 기반으로 QPM / QTM 모델을 통해 한반도 1 km 해상도의 미관측 지점 강우/기온 자료를 복원하였으며, 복원된 강우/기온 자료를 이용한 검증 과정을 통하여 QPM / QTM 모델을 이용한 복원의 정확성을 검증하였다. 최종적으로 현재기후(2000-2014년) 동안의 관측 자료를 기반으로 생산된 강우/기온 자료와 전지구 기후모델 GME 자료를 기반으로 생산된 강우/기온 자료의 Model Bias를 계산하여 관측 자료를 기반으로 한 미래 기후 전망 자료를 생산하였다.

남한 지역의 복원 강우에 대한 사례별 검증 결과 선정된 모든 사례에서 강우 정확도는 복원의 적중률이 상당히 높게 나타났다. 특히 태풍 사례에서 가장 높은 적중률을 보였으며, 모든 사례에서 오보율(FAR)이 낮게 나타났다. 북

한 지역의 복원 강우에 대한 검증 결과 모든 사례에서 남한 사례보다는 비교적 낮은 복원의 정확도와 상관성을 보였다. 복원 기온에 대한 검증 결과 검증지점에 대한 복원 기온이 실제 기온에 비하여 다소 과소 복원되는 경향이 있었다. 특히, 지형고도가 높은 지역일수록 지형 효과에 의한 기온 변화가 크게 나타나는 것을 확인하였다.

북한까지 포함한 한반도 전체 지역에 대하여 폭염, 열대야, 폭우, 강우강도의 극한 사상 변화를 전망한 결과 강우와 관련된 극한 사상의 경우 모든 시나리오에 대하여 부산 지역의 경우 수영구에 비하여 북구에서, 서울 지역의 경우 용산구에 비하여 종로구에서, 북한 양강도 지역의 경우 혜산시에 비하여 삼지연군에서 증가폭이 크게 나타날 것으로 전망되었다. 기온과 관련된 극한 사상의 경우 모든 시나리오에 대하여 부산 지역의 경우 북구에서, 서울 지역의 경우 종로구와 용산구에서 비슷하게 증가할 것으로 전망되었다.

I . Introduction

The impact of climate change on global warming is very large and widely observed. Changes in precipitation, melting of snow and ice are changing the hydrological system. Evidence of the effects of extreme climatic events (heat waves, droughts, floods, wildfires, etc.) on Earth system has been shown in the IPCC (Intergovernmental Panel on Climate Change) AR 5 Report (2013) that Earth system is vulnerable to climate change and highly exposed.

Global climate models (GCMs, General Circulation Models) have been useful in many climate research communities for long-term predictions and for future climate assessments through future climate simulation production (Lee et al., 2012). However, according to Korea Climate Change Assessment Report (2014), the climate change assessment report published by the IPCC covers the entire global or continental scale, therefore it is limited to explain the climate change phenomenon on the Korean Peninsula.

The extreme climate change prospects on the Korean Peninsula in the Korean Peninsula climate Change Prospecting Report (2013) explain that the trend of abnormal weather and extreme weather phenomena will be further heightened by the global warming in the future.

The subtropical climate zone, which is currently limited to the southern coast of Korean Peninsula in the present climate, will gradually head north in the 21st century. And also predicted a drastic increase in the extreme event, such as days of heat wave, tropical nights and heavy

rainfall days.

It is predicted that days of the heat wave will increase rapidly in the lowlands where the maximum temperature is relatively high and that the days of the tropical nights will increase in the lowlands with minimum temperature is relatively high and days of the heavy rainfall will increase significantly in most regions of Korean Peninsula.

These climate changes have a high impact on society and the economy, from climate sensitive agricultural and forestry sectors to relatively less sensitive industrial sectors (Ahn et al., 2010).

In this way, detailed climate change prediction information on the Korean Peninsula is a top priority for the Korean Peninsula to develop alternatives to the economic and industrial impacts of climate change and to improve adaptive capacity. However, it is not easy to provide adequate information on these extreme climate phenomena that are causing serious damage to city, county, and county local governments. At present, the ground observation data provided by the Korea Meteorological Administration (KMA) are scattered at an irregular interval of about 10 ~ 15 km on average, which is relatively denser than other countries (Bae, 2015). It is difficult to predict the meteorological phenomenon in the detailed region because of the low resolution to take into account the complex terrain characteristics of South Korea. In addition, there is a limit to the weather forecast and analysis of climate characteristics for the entire Korean Peninsula due to insufficient available observation data in the case of North Korea.

The demand for high resolution climate prediction data is

increasing rapidly because of the limitations of detailed regional extreme event analysis such as drought or heavy rainfall through low resolution climate prediction data (Kim et al., 2012). Especially, on Korean Peninsula where the terrain is complex, high-resolution climate prediction data considering topographic effect is required. In general, extreme weather phenomena tend to occur in a short period of time with high intensity or very local, so local and regional detailed climate information is needed.

In the previous research, National Institute of Meteorological Research (NIMR) participated as a representative group in Coupled Model Intercomparison Project Phase 5 (CMIP5) experiment for the publication of the IPCC AR5 with 13 countries including USA, Germany, and Japan, and conducted a future climate experiment based on the RCP(Representative Concentration Pathway) scenarios using the HadGEM2-AO (130 km resolution) model. In addition, the NIMR has produced detailed climate prediction data for the 50 km resolution over East Asia region, in the CORDEX project, which is being conducted by a global climate research institute for detailed regional-scale future climate projections. While this information provides useful information on future climate changes, it is difficult to predict the detailed regional climate change on the Korean Peninsula as a result of the global model prediction. Therefore, there is a limit in that the resolution is low to establish the impact of climate changes.

There are downscaling techniques to overcome the low spatial resolution of global climate models and to produce detailed regional climate data, and downscaling techniques have evolved into two

approaches, statistical downscaling and dynamical downscaling (Lee et al., 2012).

In the previous research, the PRIDE (PRISM based Downscaling Estimation) model was used to produce the temperature and precipitation data according to the high-resolution future climate change scenarios over South Korea with resolution of 1 km and analyzed the extreme indexes such as the heat wave and precipitation intensity (Kim et al., 2013).

However, this is the still only model used to study the 1 km detailed future climate prediction over South Korea. It is necessary to use another model that can overcome the limit of single model and give reliable results. Also, The statistical downscaling model is relatively simple and economical compared to the dynamical downscaling model, but has a limit in that detailed physical processes can not be considered.

Therefore, in this study, we use Quantitative Precipitation Model (QPM) and Quantitative Temperature Model (QTM) based on global climate model GME (Operational Global Model(GM) and the regional model for central Europe) data of 40 km resolution according to RCP 4.5, 8.5 scenarios to project 1 km of precipitation and temperature over Korean Peninsula. Using the QPM and QTM, we considered the physical processes of precipitation / temperature such as topographical effect, 3D wind field and humidity which are not represented by statistical downscaling model. For the topographic effect, we considered the Digital Elevation Model (DEM) topography data of 1 km resolution provided by General Bathymetric Chart of the Oceans (Fig. 1).

In addition, based on the observed data for the present climate

(2000–2014), the precipitation / temperature data of 1 km resolution over the whole region of the Korean Peninsula was restored through QPM / QTM. We verified the accuracy of restored data through verification process with verification data.

In the same way, we produced 1 km resolution precipitation / temperature simulations over Korean Peninsula region for the present climate (2000–2014), which was produced using the QPM / QTM model based on global climate model GME data. Finally, we use the Model Bias between restored data based on observations and data produced from global climate model GME data during the present climate (2000–2014) to produce future climate projections based on the observed data.

Using future precipitation / temperature prediction data of 1 km resolution according to the RCP scenarios, future climate changes and extreme event changes by city and county, which were limited by global climate models, were analyzed. We analyzed various extreme events such as heat waves, tropical nights and heavy rainfall over the whole region of Korean Peninsula including North Korea.

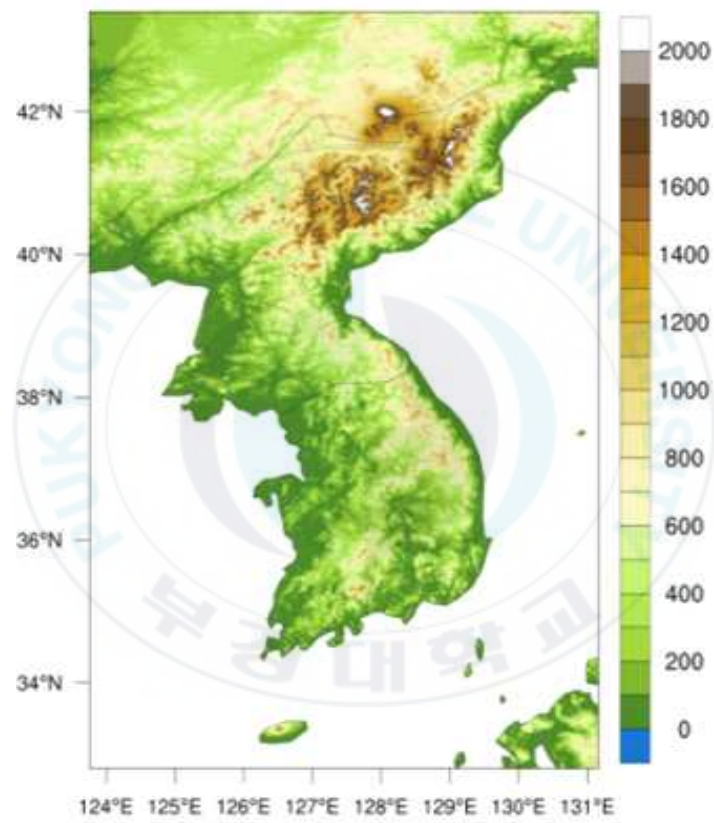


Fig. 1 DEM data to consider detailed topographic effect (Units : m)

II. Models, Data and Methodology

1. Model description

In this study, we used the QPM considering topographic effect and physics processes to produce precipitation data of 1 km resolution over Korean Peninsula according to RCP scenarios (Kim and Oh, 2010). In addition, QTM was used to produce temperature data for each region of 1 km resolution over Korean Peninsula considering the terrain effect according to regional temperature lapse rate.

1.1. Quantitative Precipitation Model(QPM)

QPM is a diagnostic model that calculates final precipitation considering small scale topographic effect. It can calculate local and regional precipitation intensity considering relatively small-scale topographic effect which is difficult to express in mesoscale model.

Also, when the existing numerical model is used to calculate the detailed scale precipitation intensity, the computation becomes complicated, so that there are many constraints because the required computational resources are considerably increased and the model integration time is long.

Therefore, it is necessary to use the precipitation diagnostic model as an alternative to the non-statistical model including the small-scale

physical processes that require a tremendous amount of computation (Misumi et al., 2001). The QPM also overcomes the disadvantages of the existing meteorological model in terms of accuracy and computational efficiency (Kim et al., 2010).

The QPM uses the terrain-following coordinate system to calculate the precipitation intensity (Kim et al., 2010). The water droplet mixing ratio Q_r , which represents the mass of water droplets containing dry mass of unit mass, is calculated by the continuity equation of Eq. 1 (Kessler, 1996).

$$\frac{\partial Q_r}{\partial t} = -u \frac{\partial Q_r}{\partial x} - v \frac{\partial Q_r}{\partial y} - w \frac{\partial Q_r}{\partial z} + \frac{1}{\rho} \frac{\partial}{\partial z} (\rho V_r Q_r) + P_1 - E_1 \quad (1)$$

Where x , y , and z are horizontal and vertical coordinates, t is time, u , v and w are wind components in horizontal and vertical direction, ρ is air density, V_r is falling velocity of water droplets, P_1 and E_1 are the condensation rate and the evaporation rate of the water droplet mixing ratio, respectively.

The physical quantity in Eq. 1 can be divided into the mesoscale field of mesoscale model and other perturbations, and can be written as Eq. 2.

$$\begin{aligned} \frac{\partial(\bar{Q}_r + Q_r')}{\partial t} = & -u \frac{\partial(\bar{Q}_r + Q_r')}{\partial x} - v \frac{\partial(\bar{Q}_r + Q_r')}{\partial y} - w \frac{\partial(\bar{Q}_r + Q_r')}{\partial z} \\ & + \frac{1}{\rho} \frac{\partial}{\partial z} [\bar{\rho} V_r (\bar{Q}_r + Q_r')] + (\bar{P}_1 + P_1') - (\bar{E}_1 + E_1') \end{aligned} \quad (2)$$

Changes in the water droplet mixing ratio over time are constant under the assumption that the atmosphere is in a steady state. Q_r' is the deviation of the mixing ratio of water droplets due to the additional condensation (P_1') and evaporation (E_1') generated by the topographic forcing. The wind component and the air density ($\bar{u}, \bar{v}, \bar{w}, \bar{\rho}$) are approximated by the values obtained from the mesoscale model and Q_r' is calculated through the parametric process on the terrain-following coordinate system.

In the method of Sinclair (1994), the rate of change between water vapor and water droplets due to the influence of the terrain is calculated, and it is assumed that the upward flow depending on the terrain is proportional to the difference of horizontal wind field and terrain. At this time, it determines the type of condensation and evaporation according to the difference (w') between the vertical wind caused by the actual terrain and produced by the terrain of mesoscale model.

Therefore, the precipitation intensity is calculated for every grid considering the process of condensation and evaporation of water vapor depending on the ascending and descending flows (Eq. 3), and the intensity of precipitation in the detailed region is finally calculated.

$$I = V_r (\bar{Q}_r + Q_r') \quad (3)$$

1.2. Quantitative Temperature Model(QTM)

QTM is a diagnostic model that calculates final temperature considering the small scale topographic effect which is difficult to expressed in the mesoscale model like the QPM. One of the important parameters for calculating local and regional temperature data according to the detailed topographic effect in QTM is temperature lapse rate.

The temperature lapse rate used at this time varies depending on the region and season, and therefore QTM uses the temperature lapse rate (Γ) for each grid instead of 6.5 °C/km, which is the environmental lapse rate (Eq. 4).

$$\Gamma_{L1-L2} = \frac{dT}{dZ} = -\frac{T_{L1} - T_{L2}}{Z_{L1} - Z_{L2}} \quad (4)$$

Where Γ_{L1-L2} represents the temperature lapse rate between $L1$ and $L2$ isobaric surfaces. T_{L1} and T_{L2} are the temperatures for the for the $L1$ and $L2$ isobaric surfaces obtained from the mesoscale model, respectively, and Z_{L1} and Z_{L2} are the geopotential height for the $L1$ and $L2$ isobaric surfaces, respectively. Therefore, the temperature lapse rate is calculated by the difference in temperature according to the geopotential height difference between two isobaric surfaces, and the temperature lapse rate for each layer is calculated at each time. Finally, to calculate the temperature according to the topographic effect, the 2 m temperature of the mesoscale model is calculated to 1000 hPa through Eq. 5.

$$T_{1000hPa} = T_i + \Gamma_i \times H_i \quad (5)$$

Where T_i is the 2 m temperature of the mesoscale model, Γ_i is the temperature lapse rate for each layer calculated above, and H_i is the topography of the mesoscale model. The calculated 1000 hPa temperature is calculated by $T_{1000hPa} \rightarrow T_{intp}$ using bilinear interpolation method. Finally, using the calculated 1000 hPa temperature, high-resolution DEM topography data, and temperature lapse rate for each layer, the 2 m temperature with detailed topographic effects is calculated (Eq. 6).

$$T_{qtm} = T_{intp} - \Gamma \times H_{dem} \quad (6)$$

2. Data

We used global model GME simulation results of 40 km resolution according to RCP 4.5 and 8.5 scenarios to produce precipitation / temperature prediction data of 1 km resolution using QPM / QTM. The future climate period predicted in this study is 2015–2100, which is 86 years, and the present climate period is 2000–2014, which is a period of 15 years.

For simulation evaluation of future climate prediction results, we used QPM / QTM to restore 1 km of detailed precipitation / temperature data over Korean Peninsula for each hour based on the observed data for the present climate (2000–2014).

We used Automatic Weather System (AWS) and Automated Synoptic Observing System (ASOS) data for 2000–2014 provided by the Korea Meteorological Agency (KMA). The distribution of used observation points is shown in Fig. 2. In the case of ground observation data, it increased steadily from 454 points in 2000 to 578 points in 2014 (Fig. 3).

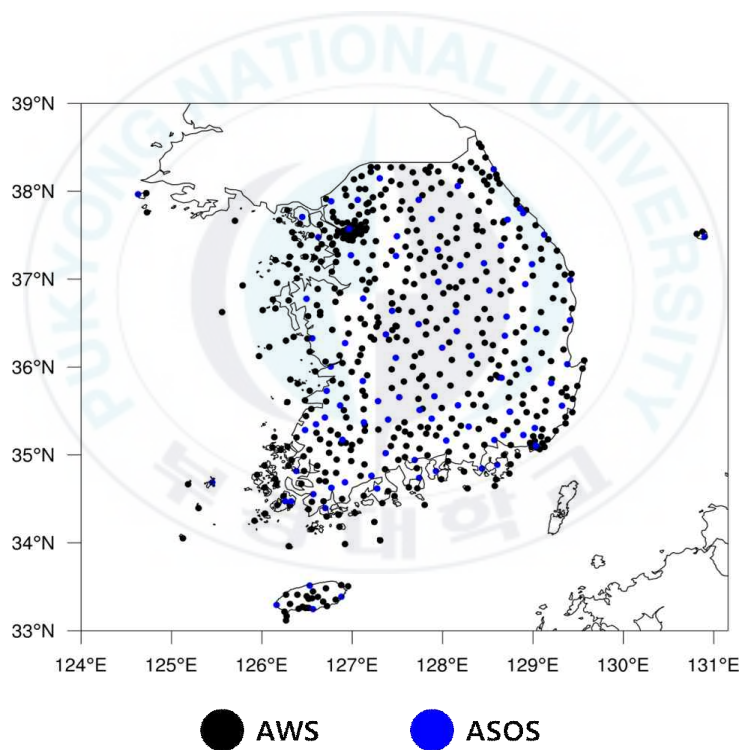


Fig. 2 Spatial distribution of AWS / ASOS observation (KMA) points (in 2014)

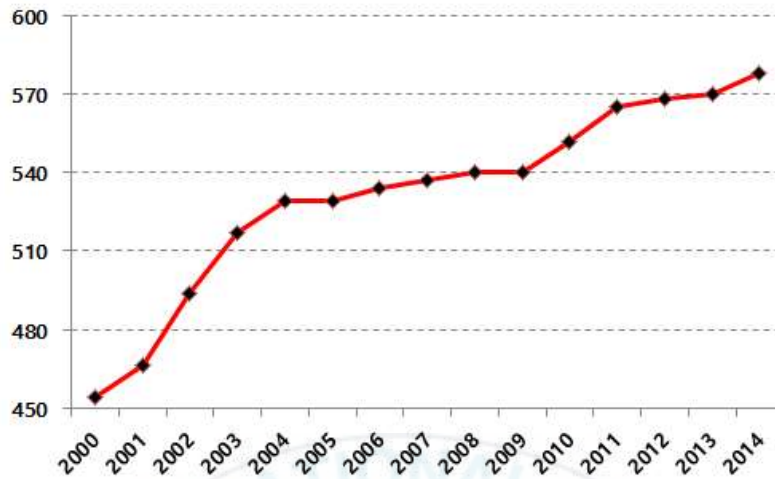


Fig. 3 Increase trend of AWS / ASOS observation (KMA) points (2000-2014)

For North Korean meteorological data, KMA provides data from 27 locations obtained through World Meteorological Organization (WMO)'s Global Telecommunication System (GTS). However, available data are lacking and precipitation is provided as cumulative precipitation, it is not suitable as data for restoration of hourly precipitation. Therefore, in the case of North Korea, the most suitable reanalysis data was selected through the verification of several reanalysis datasets, and the detailed precipitation / temperature data of 1 km resolution was restored using the selected reanalysis datasets instead of the insufficient observation data.

To select appropriate reanalysis datasets, we investigated reanalysis data and satellite data including parameters (U Wind, V Wind, Vertical Velocity, Geopotential, Relative Humidity, Air Temperature, Total Precipitation, 2 m Temperature) necessary for model execution (Table 1).

Five datasets (ERA-Interim, CFSR, GFS, MERRA, TRMM) were selected in consideration of simulation period (2000–2014), time and horizontal resolution. And verification with observation data was performed to select best dataset.

The verification was performed using the observation data located at the closest distance to the points of reanalysis datasets corresponding to South Korea region of selected data. The verification point is shown in Fig. 4.



Table 1 List of available datasets

Data	Institute	Time Interval	Horizontal Resolution	Vertical Resolution	Period
ERA-Interim	ECMWF	Vertical : 6 hr	0.75°×0.75°	60 Levels	1979–Present
		Horizontal : 12 hr			
CFSR	NCEP	6 hr	0.5°×0.5°	64 Levels	1979–2010
GFS	NCEP	6 hr	0.5°×0.5°	64 Levels	2007–Present
MERRA	NASA	Vertical : 3 hr	1.25°×1.25°	72 Levels	1979–Present
		Horizontal : 1 hr	0.667°×0.5°		
NCEP/DOE Reanalysis 2	NCEP/DOE	6 hr	2.5°×2.5°	17 Levels	1981–2010
					1979–Present
GLDAS	NASA	1 hr	0.125°×0.125°	-	1996–2007
TRMM	NASA	6 hr	0.25°×0.25°	-	1995–Present

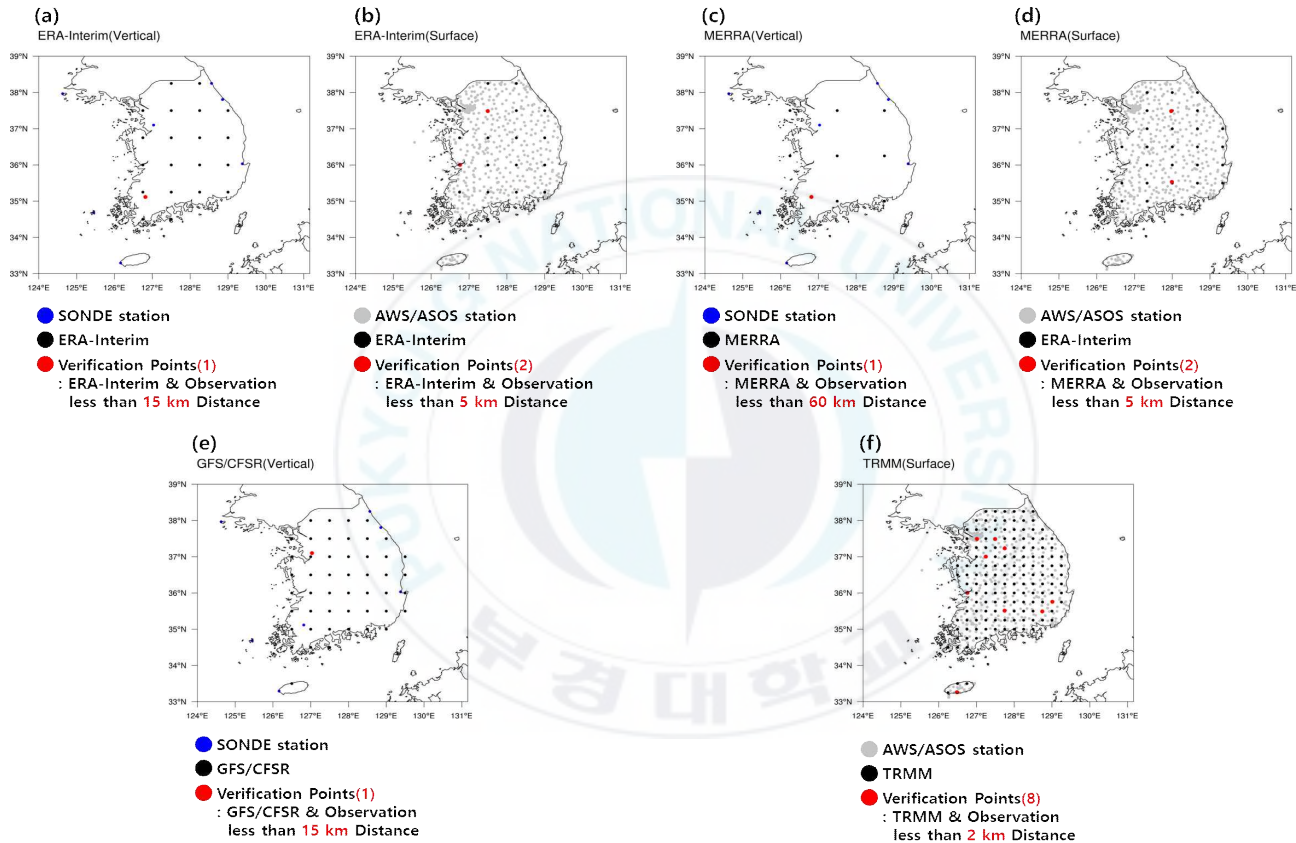


Fig. 4 Verification points of each dataset for the best dataset selection

For the ERA-Interim datasets, one point is selected within 15 km from the observation point for the verification of the vertical variables (Fig. 4a) and two points within the distance of 5 km from the observation point are selected for the verification of the surface variables (Fig. 4b). In the case of MERRA datasets, one point was selected within 60 km of the observation point for the verification of the vertical variables (Fig. 4c) and two points within 5 km from the observation point were selected for the verification of the surface variables (Fig. 4d). For the GFS data and the CFSR data, the verification point for the vertical variables was selected at a point within 15 km from the observation point (Fig. 4e). In the case of TRMM data, the verification points for the surface variables were selected from 8 points within 2 km from the observation point (Fig. 4f).

In order to select the best datasets, we conducted the correlation evaluation of four precipitation cases and the selected cases are shown in Table 2.

Table 2 Precipitation cases for selecting best datasets

Case 1	2012.07.05 ~ 2012.07.06
Case 2	2012.09.16 ~ 2012.09.17
Case 3	2013.08.22 ~ 2013.08.24
Case 4	2014.07.02 ~ 2014.07.03

Table 3 ~ 6 show the correlation evaluation results for

precipitation cases of each dataset. The results of correlation analysis of precipitation showed that TRMM correlations were higher in Case 1 and Case 4 than in MERRA reanalysis data, whereas in Case 2 and Case 3 showed higher correlations with MERRA reanalysis data. However, most of the vertical variables have high correlations with MERRA reanalysis data. Therefore, MERRA reanalysis data were used for the surface variables over North Korea region and the vertical data over Korean Peninsula, which are needed to restore the precipitation / temperature over Korean Peninsula to the present climate (2000–2014).

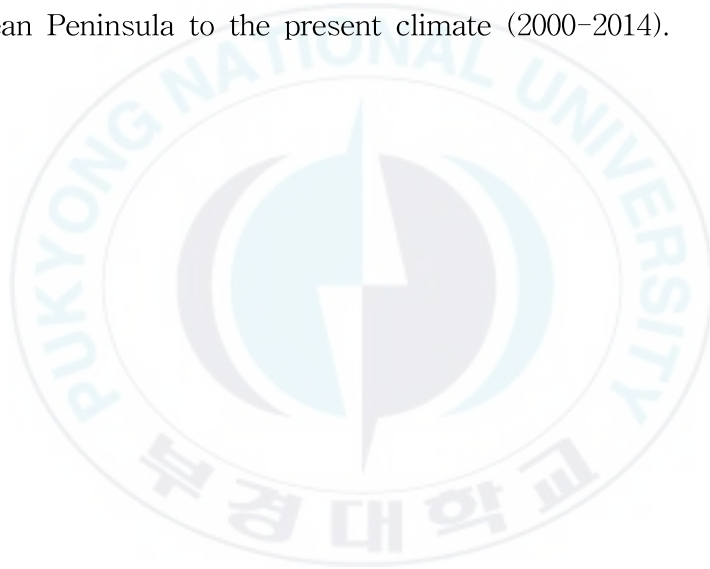


Table 3 Results of correlation analysis (Case 1)

Variable	MERRA	TRMM	ERA-Interim	GFS
Precipitation	0.52	0.75	-	-
2m Temperature	0.73	-	0.88	-
U Wind	0.95	-	0.68	0.76
V Wind	0.76	-	0.28	0.40

Table 4 Results of correlation analysis (Case 2)

Variable	MERRA	TRMM	ERA-Interim	GFS
Precipitation	0.22	0.21	-	-
2m Temperature	0.70	-	0.95	-
U Wind	0.91	-	0.76	0.70
V Wind	0.95	-	0.90	0.91

Table 5 Results of correlation analysis (Case 3)

Variable	MERRA	TRMM	ERA-Interim	GFS
Precipitation	0.27	0.24	-	-
2m Temperature	0.85	-	0.94	-
U Wind	0.94	-	0.81	0.90
V Wind	0.64	-	0.27	0.41

Table 6 Results of correlation analysis (Case 4)

Variable	MERRA	TRMM	ERA-Interim	GFS
Precipitation	0.13	0.31	-	-
2m Temperature	0.82	-	0.90	-
U Wind	0.97	-	0.79	0.72
V Wind	0.57	-	0.35	0.35

3. Methodology

3.1. Restoration of precipitation / temperature on the ungauged site

In this study, detailed precipitation / temperature data was restored over Korean Peninsula by using the method of previous study (Bae, 2015) that restored the precipitation of the ungauged site over South Korea. For this purpose, AWS / ASOS data in South Korea and MERRA Reanalysis data in North Korea, which are scattered at irregular intervals, were gridded and the precipitation intensity was finally restored considering the topographic effect. Barnes interpolation was used to convert irregularly distributed observations into gridded data. In this study, the data were converted to 10 km resolution regular grid data. This is to minimize the uncertainty in converting the irregular observation data to grid data because average distances between AWS / ASOS observations are about 10 ~ 15 km and are irregular in each region. Barnes interpolation is a method of converting irregularly distributed observation point data into constant grid point data by applying weights according to distances between observation points and grid points. DEM topography data of 1 km resolution was used to calculate the precipitation intensity through condensation and evaporation process of water vapor according to the upward flow and downward flow by the topographic effect. The wind field, relative humidity, and temperature data of MERRA reanalysis data and gridded observation

data are extracted and used as input data of QPM.

Similar to the precipitation restoration, the irregularly spaced observations were converted to gridded data using Barnes interpolation to restore the detailed temperature of the ungauged sites on the Korean Peninsula. The vertical temperature and geopotential height of the MERRA reanalysis data were used to calculate the required temperature lapse rate as input data to the QTM. Using the temperature lapse rate calculated by every grid points and DEM terrain data, we reproduced 1 km resolution temperature data for the ungauged sites considering the topographic effect.

3.2. Observation-based Future Climate prediction over Korean Peninsula

For the prediction of precipitation / temperature based on RCP scenarios, 1 km of future precipitation / temperature prediction data of 1 km over Korean Peninsula based on the observational data was generated. For this, the model bias for 2 m temperature and precipitation were calculated (Eq. 7, Eq. 8).

$$\Delta T = T_{syn} - T_{his} \quad (7)$$

$$\Delta P = P_{syn} - P_{his} \quad (8)$$

Where ΔT is the model bias for the 2 m temperature, T_{syn} is the

restored temperature based on the observed data, and T_{his} is the 1 km detailed temperature produced using the QTM based on the GME model data. Also, ΔP is the model bias for the precipitation, P_{syn} is the restored precipitation based on the observed data, and P_{his} is the 1 km detailed precipitation produced using QPM based on the GME model data.

Based on the previously calculated model bias and 1 km of precipitation / temperature data produced from GME model data, we produced 1 km detailed future precipitation / temperature prediction data over Korean Peninsula based on the observed data according to RCP scenarios (Eq. 9, Eq. 10).

$$T_{future} = \Delta T + T_{sim} \quad (9)$$

$$P_{future} = \Delta P + P_{sim} \quad (10)$$

Where T_{future} is the 1 km detailed future temperature prediction based on the observation data, ΔT is the model bias for temperature, and T_{sim} is the temperature calculated using QTM based on the GME model data. P_{future} is a 1 km detailed future precipitation prediction based on the observation data, ΔP is model bias for precipitation and P_{sim} is precipitation produced using QPM based on GME model data.

III. Verification

1. Verification of restored precipitation / temperature

In order to verify 1 km of detailed precipitation / temperature data based on the observed data, verification was carried out through elimination experiments. In the elimination experiment, there is an actual observatory, but the experiment is performed by removing the observatory randomly according to a certain criterion (Bae, 2015). In this study, we selected the verification points and restored the precipitation / temperature data of the ungauged sites using the data except the selected verification points. Next, the verification was carried out by comparing the restored precipitation / temperature data with the observation data for the verification points. To select the verification points, AWS / ASOS observation points and QPM / QTM grid points overlap at distances of 200 m or less in South Korea. In the case of North Korea, verification points were selected within a distance of 200 m from the GTS data. The selected verification points are 30 points in South Korea (Table 7) and 27 points in North Korea (Table 8). The verification point distribution is shown in Fig. 5.

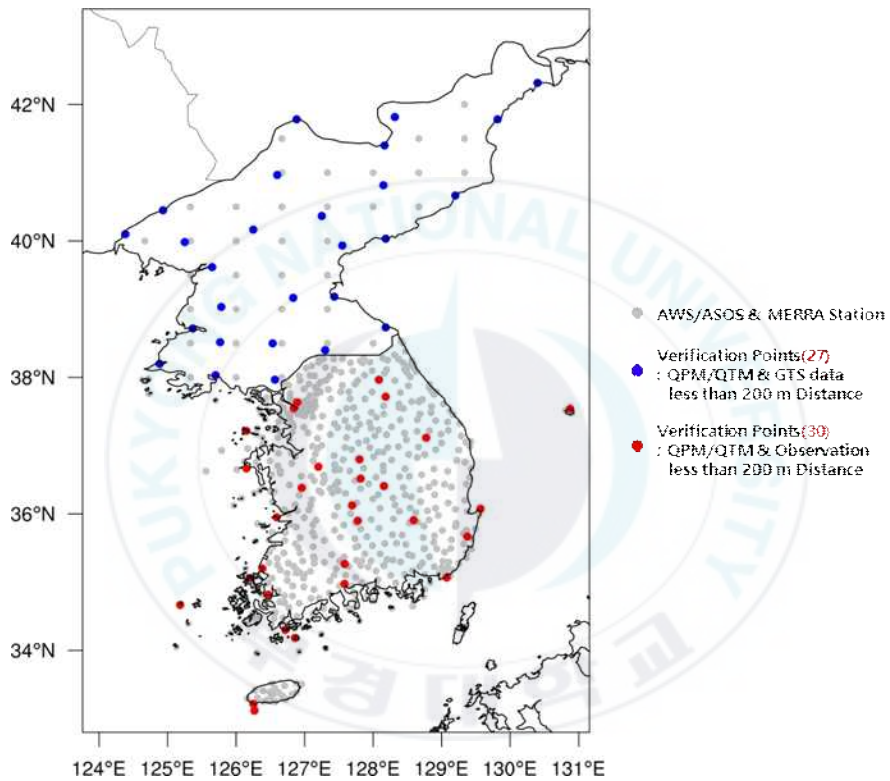


Fig. 5 Selected verification points for the verification of restored data

Table 7 Location (degrees) information for AWS / ASOS stations matching with QPM / QTM model grid points

Station number	Latitude	Longitude	Station number	Latitude	Longitude
137	36.4084	128.1574	713	34.9751	127.5826
319	37.5408	130.8746	726	33.1171	126.2673
404	37.5499	126.8425	735	35.9008	127.7755
513	37.2167	126.1500	747	34.1834	126.8585
535	37.7170	128.1827	769	35.1993	126.3834
540	37.6343	126.8917	774	34.8175	126.4662
581	37.1164	128.7742	791	35.2662	127.5838
585	37.9660	128.0834	793	33.2167	126.2500
603	36.8000	127.8000	798	34.6667	125.1833
607	36.6667	126.1500	808	36.0759	129.5667
625	36.5172	127.8167	845	35.9084	128.5907
629	36.6908	127.2005	857	34.3000	126.7173
647	36.1250	127.6924	886	35.9504	126.5911
691	36.3824	126.9586	910	35.0661	129.0742
707	35.058	126.2084	943	35.0661	129.0742

Table 8 Location (degrees) information for GTS stations matching with QPM / QTM model grid points

Station number	Latitude	Longitude	Station number	Latitude	Longitude
3	42.3167	130.4000	46	40.0333	128.1833
5	41.8167	128.3167	50	39.6167	125.6500
8	41.7833	129.8167	52	39.1667	126.8333
14	41.7833	126.8833	55	39.1833	127.4333
16	41.4000	128.1667	58	39.0333	125.7833
20	40.9667	126.6000	60	38.7167	125.3667
22	40.8167	128.1500	61	38.7333	128.1833
25	40.6667	129.2000	65	38.5167	125.7667
28	40.4500	124.9333	67	38.5000	126.5333
31	40.3667	127.2500	68	38.2000	124.8833
35	40.1000	124.3833	69	38.0333	125.7000
37	39.9833	125.2500	70	37.9667	126.5667
39	40.1667	126.2500	75	38.4000	127.3000
41	39.9333	127.5500			

1.1. Verification of restored precipitation data

In order to verify the restored precipitation data at the ungauged sites, we performed qualitative verification based on the rain contingency table. The rain contingency table is a binary partition table consisting of occurrence or non-occurrence of actual observation precipitation and restored precipitation (Table 9).

Table 9 2×2 Rain contingency table

QPM Rain		
Observed Rain	Rain	No Rain
Rain	H (Hit)	M (Miss)
No Rain	F (False)	Z (Zero)

Where H (Hit) represents the case when the restored rainfall occurs for the actual rainfall, M (Miss) represents the case when the restored rainfall does not occur for the actual rainfall, F (False) represents the case when restored rainfall occurs for the non-actual rainfall, Z (Zero) means that there is no restored rainfall for non-actual rainfall.

Based on the generated rain contingency table, rainfall accuracy (ACC), Bias Score (Bias), probability of detection (POD), False alarm ratio (FAR) were obtained and qualitative verification was performed (Eq. 9, Eq. 10, Eq. 11, Eq. 12).

$$ACC = \frac{Z+H}{N} \quad (9)$$

$$Bias = \frac{F+H}{M+H} \quad (10)$$

$$POD = \frac{H}{M+H} \quad (11)$$

$$FAR = \frac{F}{F+H} \quad (12)$$

Also, qualitative verification was performed using Root Mean Square Error (RMSE), Correlation coefficient (Eq. 13, Eq. 14).

$$RMSE = \sqrt{\frac{1}{N} \sum_{i=1}^N (F_i - O_i)^2} \quad (13)$$

$$CORR = \frac{\sum_{i=1}^N (F_i - \bar{F})(O_i - \bar{O})}{\sqrt{\sum_{i=1}^N (F_i - \bar{F})^2} \sqrt{\sum_{i=1}^N (O_i - \bar{O})^2}} \quad (14)$$

Where F is the result of restored precipitation, O is the observed data, and N is the number of verification data.

To verify the restored precipitation data, the AWS / ASOS data, which is the validation data of South Korea, were used to perform at intervals of one hour verification using data at intervals of one hour. The GTS data, which is the verification data for North Korea region, were provided as cumulative precipitation data, so we conducted the verification at 12 hour cumulative precipitation data.

For verification, three cases were selected for each of South Korea and North Korea (Table 10). Case 1, Case 2 and Case 3 of South Korea are referred to as South-Case 1, South-Case 2 and South-Case 3, respectively, and Case 1, Case 2 and Case 3 of North Korea are referred to as North-Case 1, North-Case 2 and North-Case 3, respectively.

Table 10 List of selected cases for verification of restored precipitation

	South Korea	North Korea
Case 1	2012.08.27 ~ 2012.08.30 (Typhoon Bolaven & Tembin)	2013.07.01 ~ 2013.07.02 (Heavy Rainfall)
Case 2	2011.07.26 ~ 2011.07.28 (Mt.Umyeon Landslide)	2012.07.18 ~ 2012.07.19 (Typhoon Kahnun)
Case 3	2010.07.15 ~ 2010.07.17 (Changma)	2010.07.16 ~ 2010.07.18 (Changma)

Table 11 and Table 12 show the qualitative and quantitative verification results of the restored precipitation over South Korea for the selected cases, respectively.

As a results of qualitative verification of restored precipitation in South Korea, rainfall accuracy was 0.85 or higher in all cases, and the hit rate of restoration was high. In the case of the rain contingency table of South-Case 1, which is a typhoon case, Hit was 155 times, Miss was 40 times, False was 134 times, Zero was 103 times, and Bias was 1.01, and precipitation was restored similarly with observed data. In case of South-Case 2, which is a heavy rainfall case, Hit was 206 times, Miss

was 24 times, False was 86 times, Zero was 117 times, Bias was 0.71, and there was a tendency to underestimate the occurrence of rainfall. In the case of South-Case 3, which is a rainy season case, Hit showed 239 times, Miss was 70 times, False was 108 times, Zero was 231 times, and Bias was 0.91, showing a slight underestimation of rainfall occurrence. Probability of detection, which represents the accuracy ratio of restored precipitation, was higher than 0.6 in all cases, and the highest hit rate was 0.87 in typhoon cases in particular. The false alarm ratio was 0.15 or less in all cases, and the accuracy of precipitation was high in all cases. As a result of quantitative verification of the restored precipitation in South Korea, the average precipitation per hour was about 0.1 ~ 0.2 mm in all cases. The RMSE was relatively high in the Mt. Umyeon landslide case (South-Case 2), but the CORR was 0.85 or more in all cases.

Table 11 Results of Qualitative verification of restored precipitation over South Korea

	South Korea(1 hourly)		
	Case 1	Case 2	Case 3
ACC	0.92	0.89	0.89
BIAS	1.01	0.71	0.91
POD	0.87	0.63	0.77
FAR	0.14	0.11	0.15

Table 12 Results of Quantitative verification of restored precipitation over South Korea

	South Korea(1 hourly)		
	Case 1	Case 2	Case 3
AVE (Observation / QPM)	5.49 / 5.33	6.18 / 6.02	3.48 / 3.51
STD (Observation / QPM)	6.35 / 5.92	9.20 / 6.97	4.04 / 3.40
RMSE	2.05	6.03	0.54
CORR	0.95	0.75	0.78

Table 13 and Table 14 show the qualitative and quantitative results of the restored precipitation in North Korea for the selected cases respectively. As a result of qualitative verification of restored precipitation in North Korea, the accuracy of precipitation was over 0.6 in all cases. In the case of North-Case 1, which was a heavy rainfall case, Hit was 155 times, Miss was 40 times, False was 134 times, Zero was 103 times, and Bias was 1.48, showing a tendency to overestimate the occurrence of precipitation. In the case of North-Case 2, which is a typhoon case, Hit was 206 times, Miss was 24 times, False was 86 times, Zero was 117 times, and Bias was 1.27, showing a tendency to overestimate the occurrence of precipitation. Next, in the case of the North-Case 3, which is a changma case, Hit was 239 times, Miss was 70 times, False was 108 times, Zero was 231 times and Bias was 1.12, showing overestimation similar to other cases.

The probability of detection (POD) of restored precipitation for actual precipitation was higher than 0.75 in all cases, and the highest hit

rate was 0.90 in typhoon cases in particular. However, the false alarm ratio (FAR) was relatively higher in all cases than in South Korea. As a result of quantitative verification of restored precipitation in North Korea, the restoration accuracy is relatively low in all cases than the South Korea cases. This may be due to the uncertainty of the MERRA reanalysis data used as the initial precipitation data in North Korea and the low reliability of the GTS data used for verification (Cha et al., 2012).

Table 13 Results of Qualitative verification of restored precipitation over North Korea

	North Korea(12 hourly)		
	Case 1	Case 2	Case 3
ACC	0.60	0.75	0.73
BIAS	1.48	1.27	1.12
POD	0.79	0.90	0.77
FAR	0.46	0.29	0.31

Table 14 Results of Quantitative verification of restored precipitation over North Korea

	North Korea(12 hourly)		
	Case 1	Case 2	Case 3
AVE (Observation / QPM)	34.44 / 21.90	32.95 / 20.59	23.70 / 18.98
STD (Observation / QPM)	22.97 / 15.08	21.91 / 9.57	17.35 / 10.61
RMSE	28.47	24.10	18.13
CORR	0.14	0.34	0.29

1.2. Verification of restored temperature data

In order to verify the accuracy of the restored temperature data on the ungauged sites, quantitative verification of case and whole period was performed (Table 15).

Table 15 List of selected cases for restored temperature verification

Case 1	2014.08.01 ~ 2014.08.02 (Heat Wave)
Case 2	2011.01.16 ~ 2011.01.17 (Cold Wave)

Table 16 shows the results of quantitative verification of the restored temperature for each selected case. As a result of the quantitative verification on the restored temperature, the RMSE was 4.64 in the case of the cold wave, and the error for the low temperature was larger than the error for the high temperature.

Also, the CORR was 0.7 or higher in all cases, and the hit rate of restoration was high, but the error decreased and the correlation tended to be higher when the gridded temperature lapse rate was applied.

Table 16 Results of quantitative verification of restored temperature by cases (Unapplied : Gridded temperature lapse rate unapplied, Applied : Gridded temperature lapse rate applied)

Lapse Rate	Unapplied			Applied		
	AVE	RMSE	CORR	AVE	RMSE	CORR
Case 1	27.0	2.30	0.81	26.7	2.31	0.83
Case 2	-10.1	4.79	0.76	-12.3	4.64	0.79

In order to verify the restored temperature data for the ungauged sites, the data of 1 hour intervals were analyzed in both South Korea and North Korea. Table 17 shows the mean error between the restored temperature and the actual temperature for the entire period (2000–2014), depending on the difference between the difference between the actual altitude of the observatory and the DEM terrain altitude. For most of the verification points, the restored temperature tended to be somewhat underestimated, compared to the actual temperature. Especially, at the site where the altitude of the DEM terrain is 250 ~ 400 m higher than the AWS / ASOS terrain elevation (735, 791, 943 sites), the restored average temperature is lower than the actual average temperature. As a result, it can be seen that the higher the altitude, the greater the temperature change due to the topographic effect.

Table 18 shows the results of monthly quantitative verification of the restored temperature for the entire period (2000–2014). In South

Korea, correlation coefficient was over 0.95 for all periods, and the monthly average error between restored and actual observation temperature was 0.29 ~ 0.53 °C, which was somewhat overestimated. Overall, the accuracy of restored temperature was high regardless of the season.

As a result of monthly temperature verification in North Korea, the correlation coefficient was 0.74 ~ 0.83, which shows that the accuracy of restored temperature is higher than that of precipitation. Monthly mean error generally shows a negative mean error, which seems to be the result of considering the detailed topographic effect on the high terrain region of North Korea.

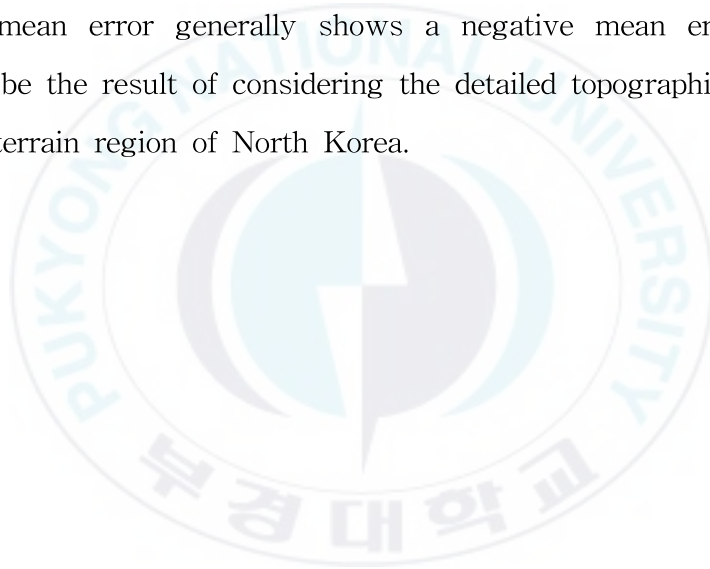


Table 17 Results of quantitative verification of restored temperature by verification points

Station number	DEM Height(m)	Observation Height(m)	Height difference(m)	Average error(℃)
137	123.0	131.3	-8.3	-0.4
319	52.0	138.7	-86.7	-1.5
404	36.0	78.4	-42.4	-0.1
535	312.0	298.3	13.7	-0.6
540	47.0	87.4	-40.4	1.0
581	528.0	405.7	122.3	-0.8
585	253.0	302.5	-49.5	-0.5
603	323.0	165.0	158.0	-0.2
625	344.0	233.4	110.6	-0.2
629	106.0	53.8	52.2	0.3
735	671.0	291.9	379.1	-3.2
791	484.0	142.7	341.3	-2.6
943	375.0	89.7	285.3	-2.1

Table 18 Results of monthly quantitative verification of restored temperature

Month	South Korea		North Korea	
	Correlation	Average Error(℃)	Correlation	Average Error(℃)
Jan	0.97	0.47	0.77	-1.89
Feb	0.98	0.42	0.81	-1.08
Mar	0.98	0.41	0.83	-0.25
Apr	0.97	0.37	0.79	0.34
May	0.97	0.29	0.74	0.23
Jun	0.96	0.29	0.74	-0.38
Jul	0.95	0.32	0.76	-0.32
Aug	0.95	0.41	0.82	-0.78
Sep	0.96	0.43	0.83	-1.56
Oct	0.97	0.45	0.82	-2.04
Nov	0.97	0.53	0.82	-2.29
Dec	0.97	0.52	0.79	-2.42

2. Evaluation of Simulation

The simulation results of the detailed precipitation / temperature data produced by QPM / QTM using the GME model result data's initial data were evaluated. The simulations were evaluated through seasonal differences between restored 1 km precipitation / temperature data from observations and present climate data based on GME model data for the same period.

Fig. 6 shows seasonal model bias between restored 1 km of detailed precipitation data based on observations and detailed precipitation data generated from GME model data.

In the case of precipitation, there was a tendency to overestimate over all seasons. In particular, the JJA period (Fig. 6b) overestimated precipitation over the entire Korean Peninsula. The tendency of overestimation was large along North Korea's Rangnim mountains and South Korea's Taebaek mountains.

The seasonal model bias between restored 1 km of detailed temperature data based on observations and detailed temperature data from GME model data is shown in Fig. 7.

In the case of temperature, there was a tendency to underestimate in North Korea except Hwanghae in all seasons. In particular, there was a tendency to underestimate in Mt. Baekdu region.

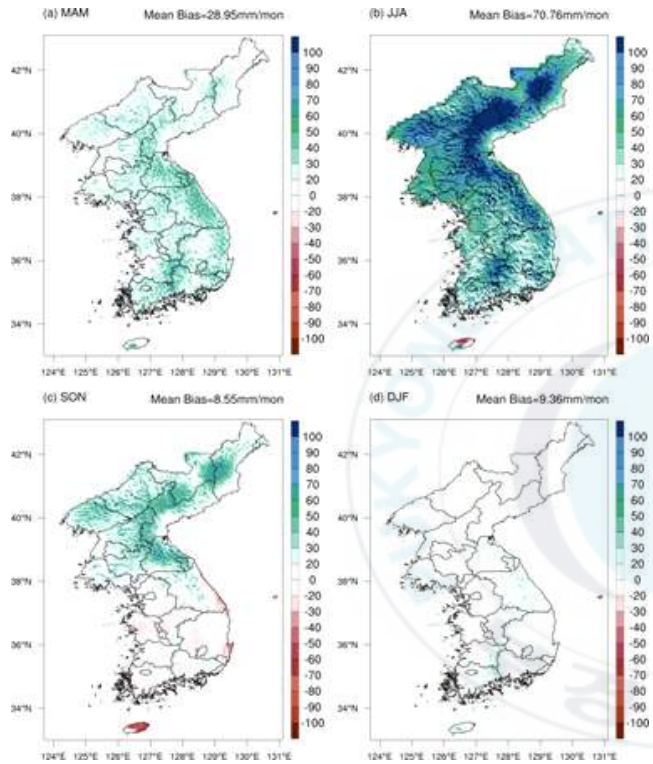


Fig. 6 Model Bias of seasonal precipitation between the restored data and produced data from GME model

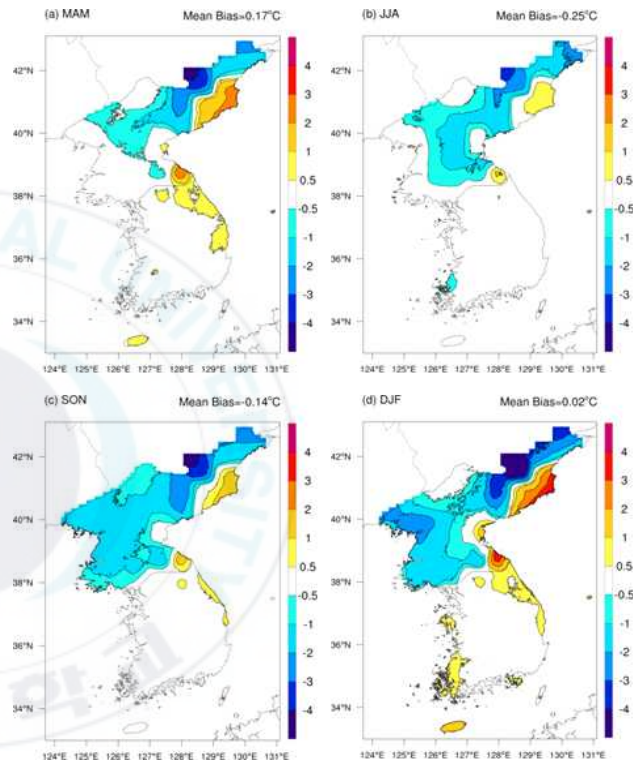


Fig. 7 Model Bias of seasonal temperature between the restored data and produced data from GME model

IV. Results

1. Prediction of detailed Future Climate over Korean Peninsula

In this study, to analyze the detailed future climate change of Korean Peninsula according to RCP scenarios, Jongro and Yongsan in Seoul, Suyoung and Buk in Busan, Hyesan and Samjiyon in Yanggang were selected (Fig. 8).

The mean altitude of each region is higher in Yongsan than in Jongro in Seoul, higher in Buk than in Suyoung in Busan and higher in Samjiyon than in Hyesan in Yanggang. We analyzed the 10-year average and monthly average precipitation / temperature changes for each selected region.

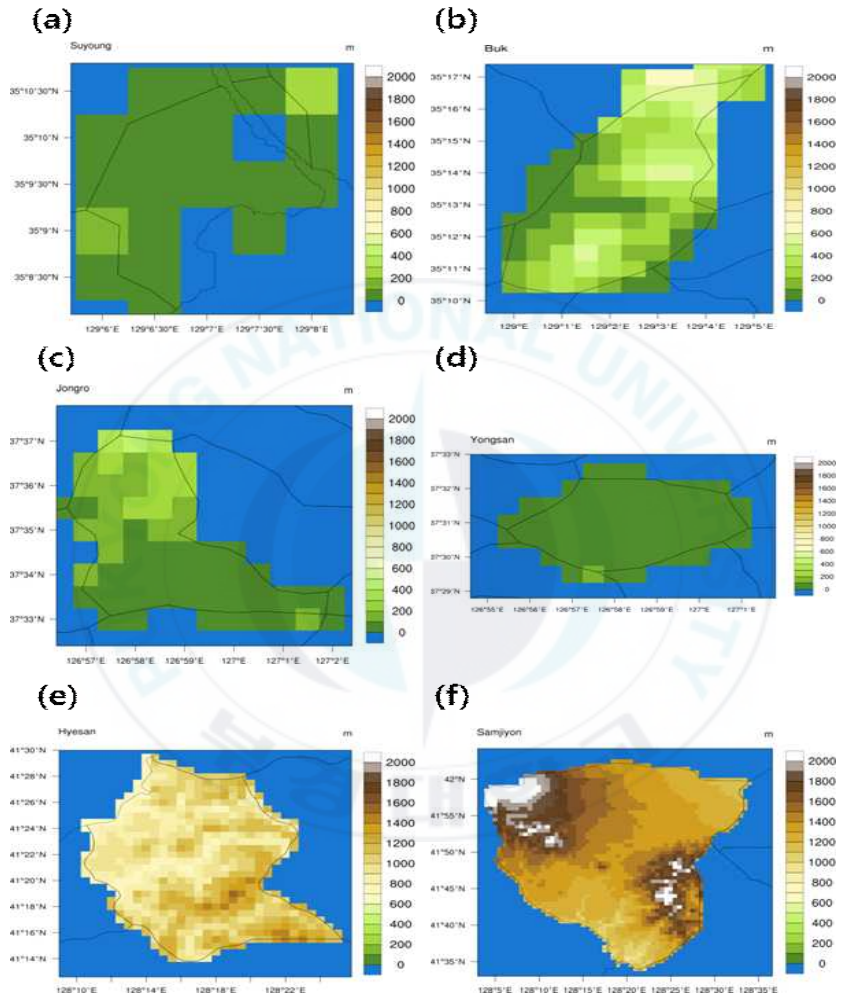


Fig. 8 Selected regions for detailed analysis of the future climate changes over Korean Peninsula

1.1. Prediction of future precipitation change

Through the graph of 10-year average precipitation change and the graph of monthly mean precipitation change, detailed precipitation changes by 1 km of detailed precipitation data over Korean Peninsula based on observational data were investigated according to the RCP scenarios.

Looking at the 10-year average precipitation change, it is predicted that the precipitation will increase from 2030 to 2090 in Seoul (Jongro, Yongsan) in RCP 8.5 scenario. It is predicted that the increase in precipitation will increase with the end of the 21st century (Fig. 9). In Seoul, it is expected that the increase in precipitation will be relatively large in Jongro than in Yongsan. In the case of Busan (Suyoung, Buk), the precipitation is expected to increase from the 2030s to 2090s, and it is expected to increase relatively in 2030s and 2040s compared to other regions.

In Busan, the increase of precipitation in Buk was expected to be larger than that in the Suyoung. As with the Seoul and Busan regions, the precipitation in Yanggang is expected to increase from the 2030s to the 2090s. In Yanggang (Hyesan, Samjiyon), the increase of precipitation in Hyesan was larger than that of Samjiyon from 2030s to 2060s, but the increase of precipitation from Samjiyon was expected to be larger than Hyesan from the 2070s.

In the RCP 4.5 scenario, it is predicted that the precipitation change will be larger in all regions than in the RCP 8.5 scenario. Also,

unlike the RCP 8.5 scenario, when the increase in precipitation is noticeable, the overall increase in precipitation is expected to be low in RCP 4.5 scenario, and will decrease in some periods (Fig. 10).

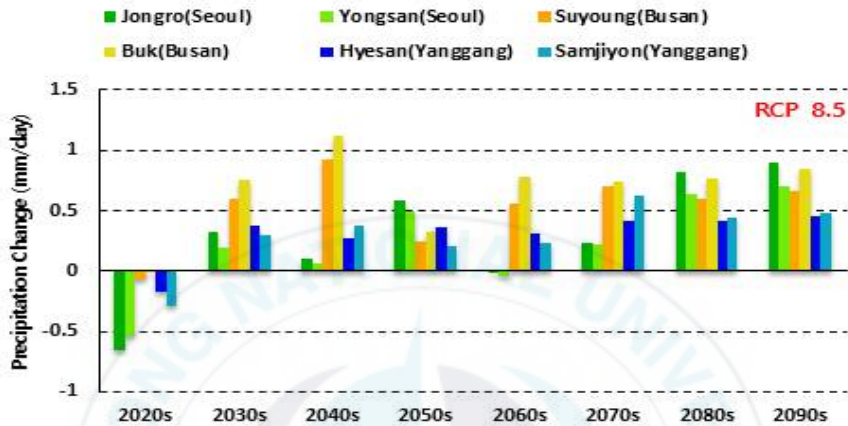


Fig. 9 Graph of regional detailed precipitation changes (decadal-average) based on the RCP 8.5 scenario over Korean Peninsula

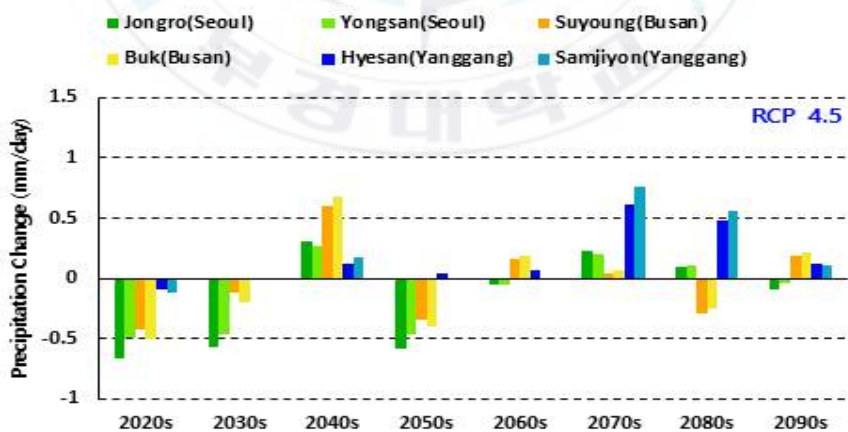


Fig. 10 Graph of regional detailed precipitation changes (decadal-average) based on the RCP 4.5 scenario over Korean Peninsula

Looking at the monthly average precipitation change, it is predicted that the precipitation will decrease significantly in June and the precipitation will increase greatly in July in both RCP 8.5 and 4.5 scenarios in Seoul (Fig. 11, Fig. 12). In addition, precipitation is expected to increase during the winter season (DJF) over Korea Peninsula. In particular, in case of RCP 8.5 scenario, both Jongro and Yongsan are expected to increase by more than 0.5 mm/day, and the increase is expected to be more in Jongro than in Yongsan. For the RCP 4.5 scenario, the increase of precipitation was smaller than in the RCP 8.5 scenario, but the tendency to increase in winter (DJF) precipitation was remarkable.

In Busan, precipitation is expected to increase overall in the RCP 8.5 scenario, and precipitation is expected to increase significantly in June and July (Fig. 13, Fig. 14). However, in the case of the RCP 4.5 scenario, the changes of precipitation were large. Although the increase is smaller than the RCP 8.5 scenario, precipitation has increased in June and July, and precipitation is expected to increase significantly in April. And precipitation is expected to decrease in May, August, October and December.

In the case of Yanggang, precipitation is expected to increase overall except for July, August, and September of Samjiyon in RCP 8.5 scenario. In both scenarios, Hyesan and Samjiyon are expected to increase by about 0.5 mm/day excluding July, August and September (Fig. 15, Fig. 16). For the RCP 4.5 scenario, precipitation is expected to increase except for April, August and September, and the increase of

precipitation is expected to be relatively large in October.

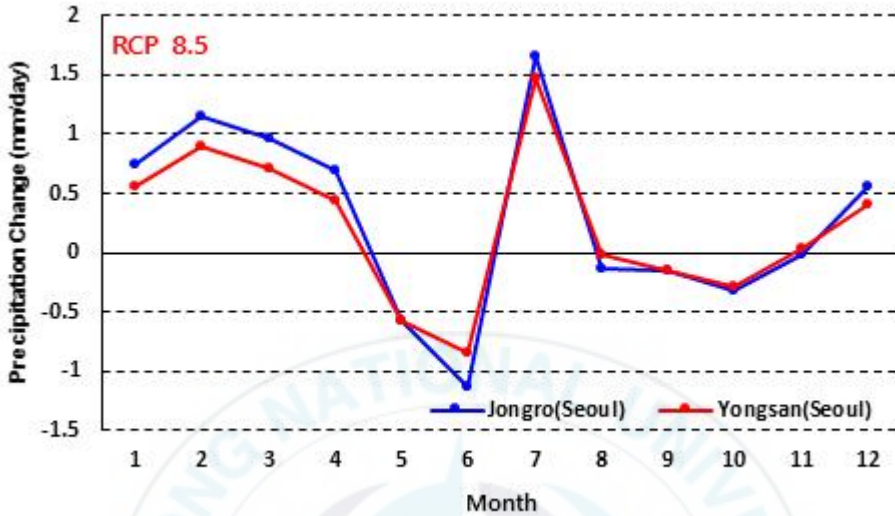


Fig. 11 Graph of detailed precipitation changes (monthly-average) based on the RCP 8.5 scenario over Seoul regions

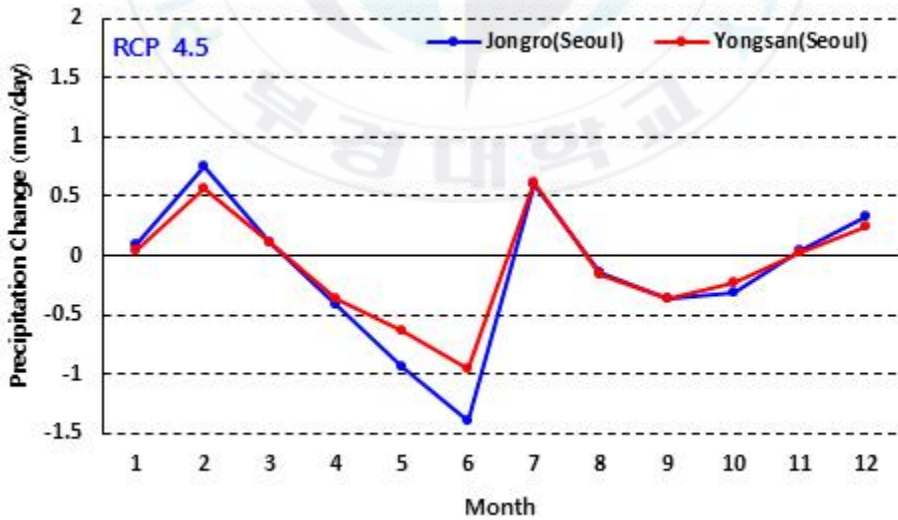


Fig. 12 Graph of detailed precipitation changes (monthly-average) based on the RCP 4.5 scenario over Seoul regions

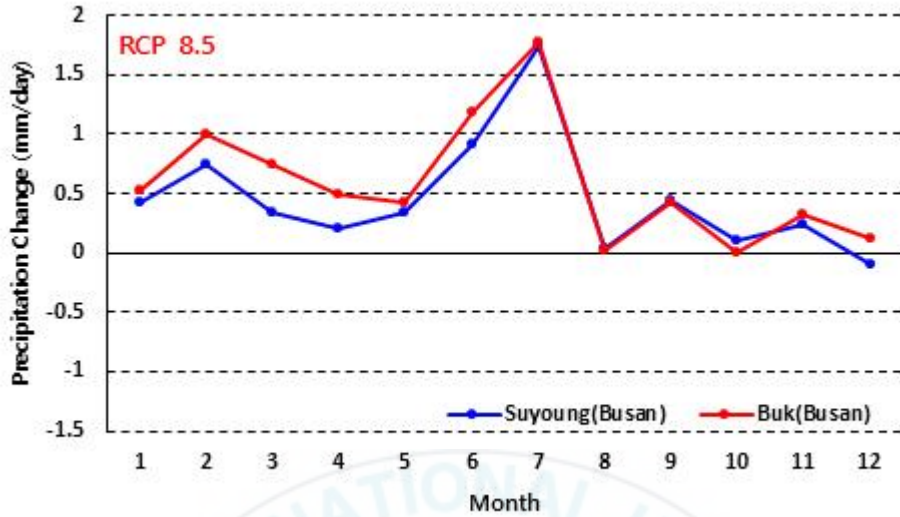


Fig. 13 Graph of detailed precipitation changes (monthly-average) based on the RCP 8.5 scenario over Busan regions

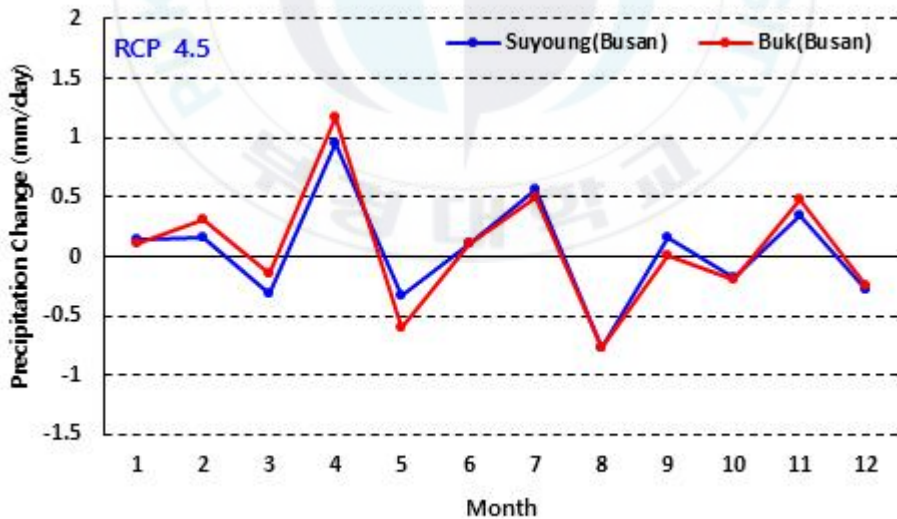


Fig. 14 Graph of detailed precipitation changes (monthly-average) based on the RCP 4.5 scenario over Busan regions

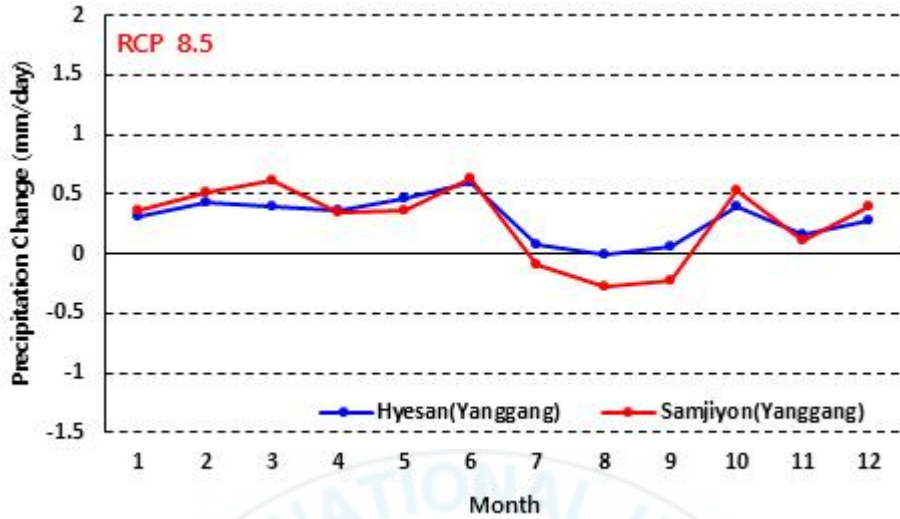


Fig. 15 Graph of detailed precipitation changes (monthly-average) based on the RCP 8.5 scenario over North Korea regions

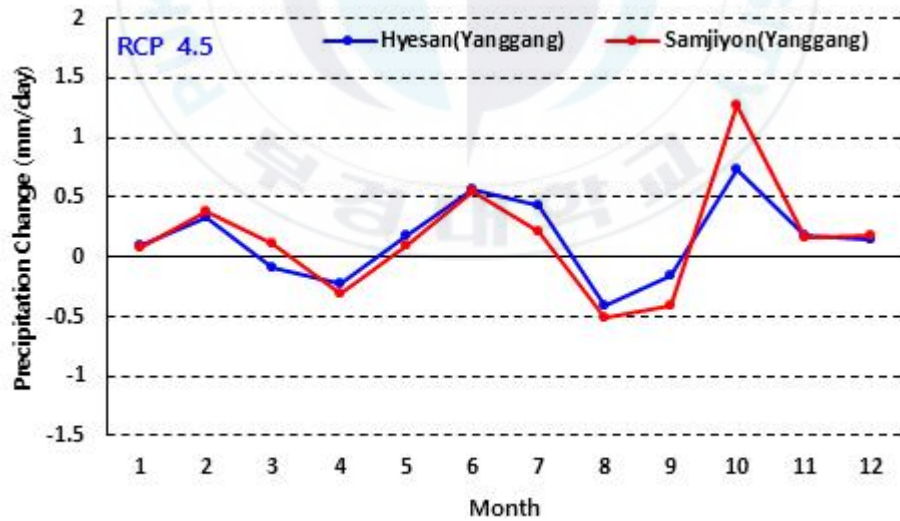


Fig. 16 Graph of detailed precipitation changes (monthly-average) based on the RCP 4.5 scenario over North Korea regions

1.2. Prediction of future temperature change

In this chapter, through the graph of 10-year average temperature change and the graph of the monthly average temperature change, detailed temperature changes by the 1 km temperature data over Korean Peninsula based on the RCP 8.5 and 4.5 scenarios were investigated.

In the case of RCP 8.5 scenarios, the temperature is expected to increase steadily from the 2020s to the 2090s. In the 2090s, it is expected to increase by about 4 °C in Busan, about 4.5 °C in Seoul and 5 °C in Yanggang. In the case of Seoul, the increase of temperature is similar to that of Korean Peninsula, while the increase of temperature in Busan is expected to be smaller than in other regions. In the case of Yanggang, the temperature is expected to increase by 0.2 ~ 0.5 °C more than other regions (Fig. 17).

For the RCP 4.5 scenario, the temperature was expected to increase with time, but the increase of temperature was expected to be smaller than the RCP 8.5 scenario (Fig. 18). In the 2090s, the temperature in Busan is expected to increase by about 2.2 °C, in Seoul by 2.5 °C, and in Yanggang by about 2.5 °C. In all scenarios, the increase of temperature in the higher latitudes tended to be larger in general.

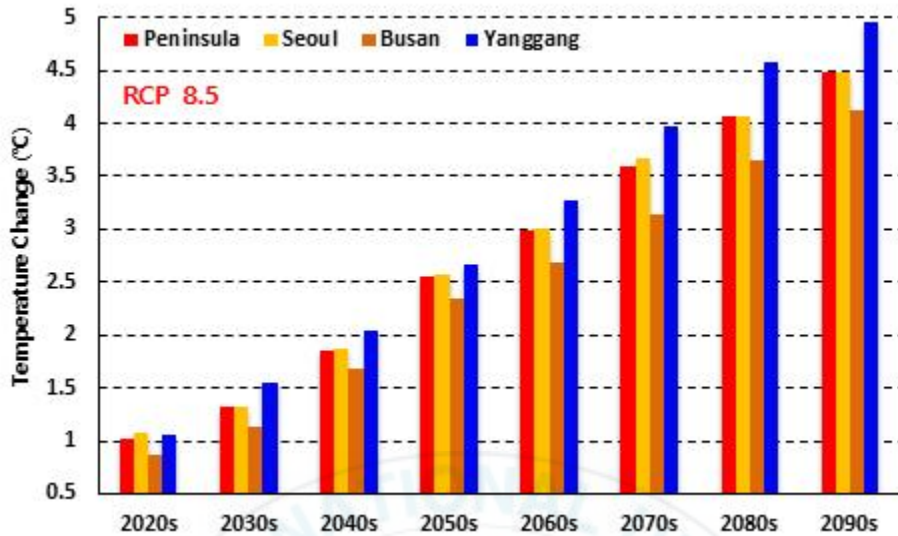


Fig. 17 Graph of regional detailed temperature changes (decadal-average) based on the RCP 8.5 scenario over Korean Peninsula

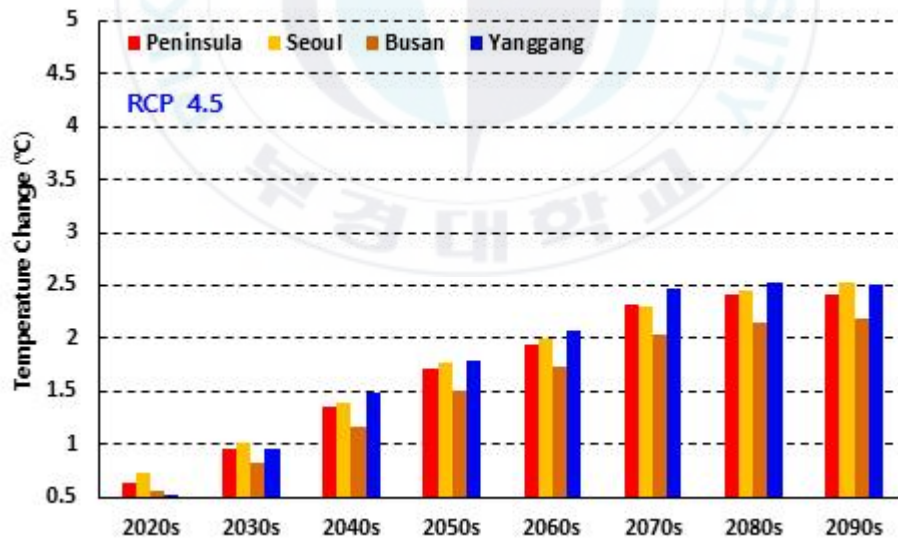


Fig. 18 Graph of regional detailed temperature changes (decadal-average) based on the RCP 4.5 scenario over Korean Peninsula

In case of RCP 8.5 scenario, the increase of temperature in Busan was relatively low compared to other regions, and the increase of temperature in Yanggang was relatively higher than in other regions (Fig. 19). During the summer (JJA) period over Korean Peninsula, the increase of temperature is expected to be smallest and the increase of temperature is expected to be the highest during the winter (DJF) period. In addition, it is expected that the difference in increase of temperature between Yanggang, which shows the highest temperature increase during winter and Busan, which shows the lowest temperature increase will be about 1.5 °C difference.

In winter, the increase of temperature was higher in the higher latitudes, and it is expected that the difference of increase of temperature by latitude will tend to be relatively small in summer.

For the RCP 4.5 scenario, the increase of temperature was expected to be highest during the winter (DJF) period over Korean Peninsula, similar to the RCP 8.5 scenario (Fig. 20). However, the overall increase of temperature was smaller than in the RCP 8.5 scenario. It is also expected that the difference in temperature between the Yanggang, where the greatest temperature increases during the winter period, and Busan, where the maximum temperature increase is small, will be about 1.0 °C. As in the RCP 8.5 scenario, it is predicted that the higher the latitude, the greater the increase of temperature in winter. Also in summer, the increase of temperature was the largest in Seoul in the middle of Korean Peninsula, but the difference in the temperature

increase by latitude is expected to be relatively small compared to the winter season.

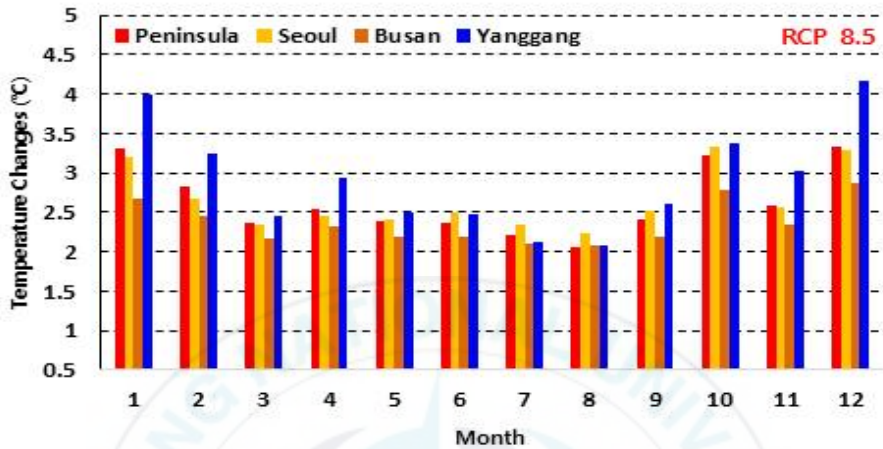


Fig. 19 Graph of regional detailed temperature changes (monthly-average) based on the RCP 8.5 scenario over Korean Peninsula

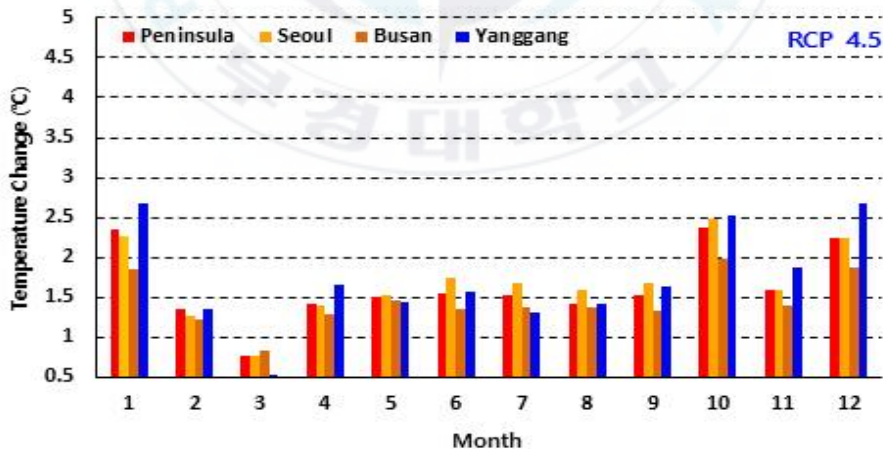


Fig. 20 Graph of regional detailed temperature changes (monthly-average) based on the RCP 4.5 scenario over Korean Peninsula

2. Changes of extreme events

In order to analyze the detailed future extreme event changes over Korean Peninsula, the extreme event changes for the far-future (2086–2100) were analyzed based on the present climate (2000–2014). For each region, changes of heavy rainfall days precipitation intensity were analyzed. In case of temperature, we analyzed the changes in the days of heat wave and tropical nights.

2.1. Changes of extreme events related to precipitation

In order to analyze the changes of extreme event related to detailed regional precipitation for the far-future (2086–2100) over Korean Peninsula, we analyzed the changes of heavy rainfall days and precipitation intensity. In this case, heavy rainfall days based on cases when daily precipitation exceeds 50 mm were selected.

Fig. 21 and Fig. 22 shows the prediction of the number of days of heavy rainfall over detailed regions of Korean Peninsula according to the RCP 8.5 and 4.5 scenarios, respectively. For all scenarios in Busan, the increase of heavy rainfall days in Buk (Fig. 21b, Fig. 22b) was expected to be higher than that of the Suyoung (Fig. 21a, Fig. 22a). Also in Seoul, the increase of heavy rainfall days is expected to be larger in Jongro (Fig. 21c, Fig. 22c) than in Yongsan (Fig. 21d, Fig. 22d). It is predicted that the number of days of heavy rainfall will increase in Samjiyon (Fig. 21f, Fig. 22f) compared to Hyesan (Fig. 21e, Fig. 22e) in

Yanggang. In particular, it is expected that the highest number of heavy rainfall days will be higher in Mt. Baekdu in Samjiyon than in other regions. Also, the increase of the number of heavy rainfall days in all regions is expected to be relatively high in the RCP 8.5 scenario compared to the RCP 4.5 scenario. Precipitation intensity shows an increase similar to the heavy rainfall days (Fig. 23, Fig. 24). The increase of precipitation intensity is expected to be larger in Buk than in Suyoung in Busan, larger in Jongro than in Yongsan in Seoul, and larger in Samjiyon than in Hyesan in Yanggang. Especially, it is expected that the precipitation intensity is high near Mt. Geumjeong in Buk in Busan, near Mt. Bukhan in Jongro in Seoul, and near Mt. Baekdu in Samjiyon. Also, as with the heavy rainfall days, the increase of precipitation intensity in all regions is expected to be relatively high in the RCP 8.5 scenario compared to the CP 4.5 scenario. Overall, in all scenarios, the increase of precipitation-related extreme events is expected to be large in areas with high average altitude.

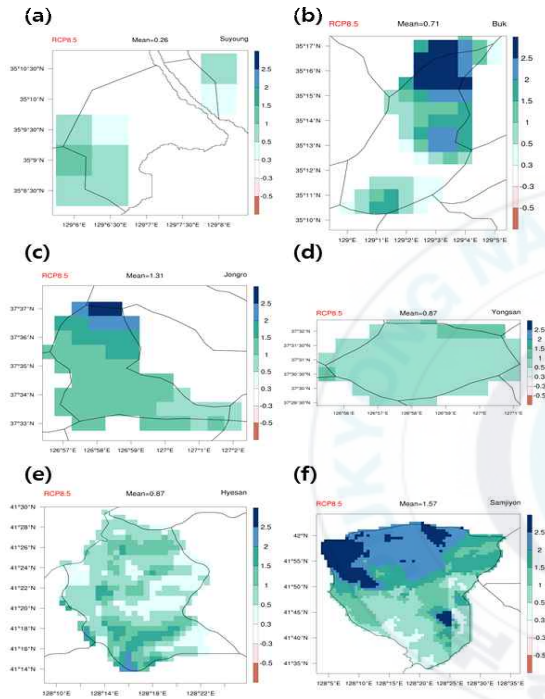


Fig. 21 Detailed regional heavy-rainfall prediction for the far-future climate based on the RCP 8.5 scenario over Korean Peninsula

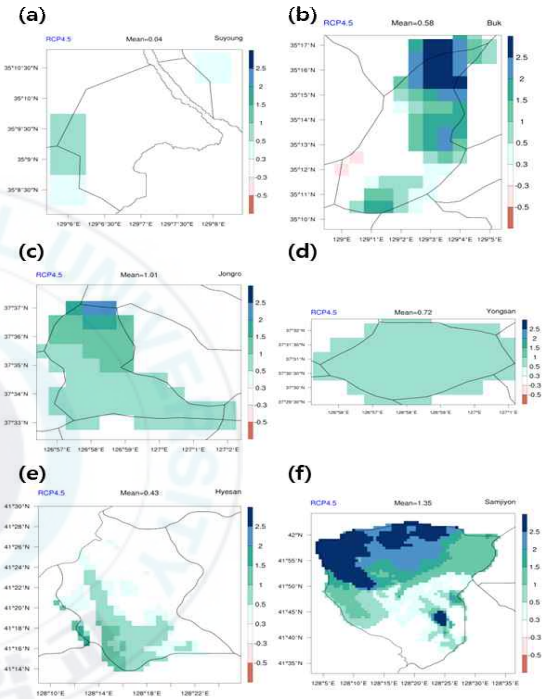


Fig. 22 Detailed regional heavy-rainfall prediction for the far-future climate based on the RCP 4.5 scenario over Korean Peninsula

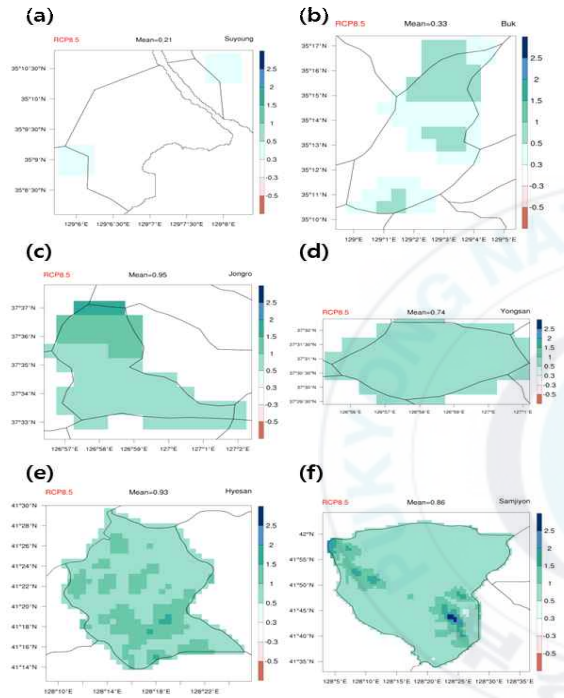


Fig. 23 Detailed regional precipitation intensity prediction for the far-future climate based on the RCP 8.5 scenario over Korean Peninsula

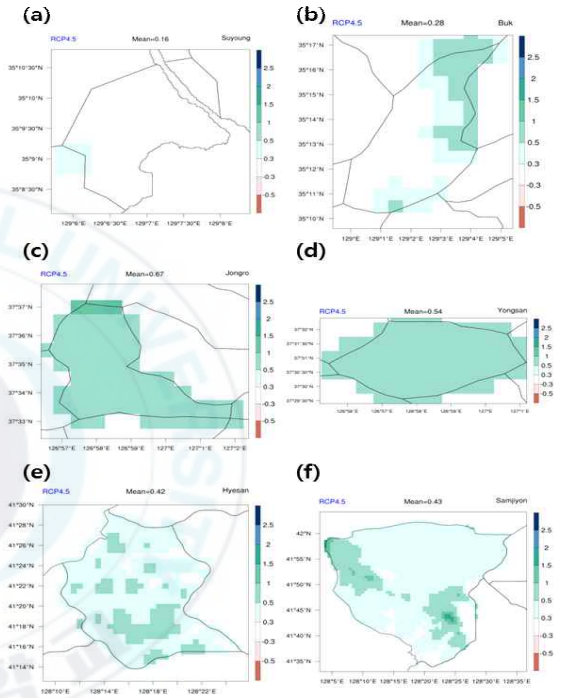


Fig. 24 Detailed regional precipitation intensity prediction for the far-future climate based on the RCP 4.5 scenario over Korean Peninsula

2.2. Changes of extreme events related to temperature

In order to analyze the extreme event changes related to the detailed regional temperature for the far-future(2086–2100) over Korean Peninsula, the number of days of heat wave and tropical nights were analyzed. In the case of the number of heat waves, the case was selected when the maximum temperature exceeded 35 °C for 2 days or more, and case of tropical nights was selected when the maximum temperature was over 30 °C and the minimum temperature was 25 °C or more.

Fig. 25 and Fig. 26 shows the predictions of the number of days of heat waves over detailed regions of Korean Peninsula according to the RCP 8.5 and 4.5 scenarios, respectively. For all scenarios, it is expected that the increase of heat wave in Buk (Fig. 25b, Fig. 26b) is higher than that of Suyoung (Fig. 26a, Fig. 26b) in Busan, but the increase of heat wave in Busan seems to be lower than other regions. In the case of Seoul, it is expected that the heat wave will increase in Yongsan (Fig. 25d, Fig. 26d) compared to Jongro (Fig. 25c, Fig. 26c) in Seoul. And in Yanggang, it is predicted that the days of heat waves will increase more in Hyesan (Fig. 25e, Fig. 26e) than Samjiyon (Fig. 25f, Fig. 26f).

Fig. 27 and Fig. 28 shows the prospect of the number of tropical nights over the detailed region of Korean Peninsula according to the RCP 8.5, 4.5 scenarios, respectively. For all scenarios in Busan, it is expected that the number of tropical night days in Buk will increase more in Suyoung, but the increase of tropical night days is relatively small in the RCP 4.5 scenario. And in Seoul, in Yongsan showed a

relatively higher number of tropical night days than in Jongro. It is expected that the tropical nights days will increase in Samjiyon than in Hyesan. In particular, the tropical night days in Samjiyon near Mt. Baekdu and Samjiyon Lake is expected to be small. Overall, in all scenarios, the increase of temperature related extreme events was expected to be small in regions with high altitude, which is in contrast to the changes of precipitation related extreme events.



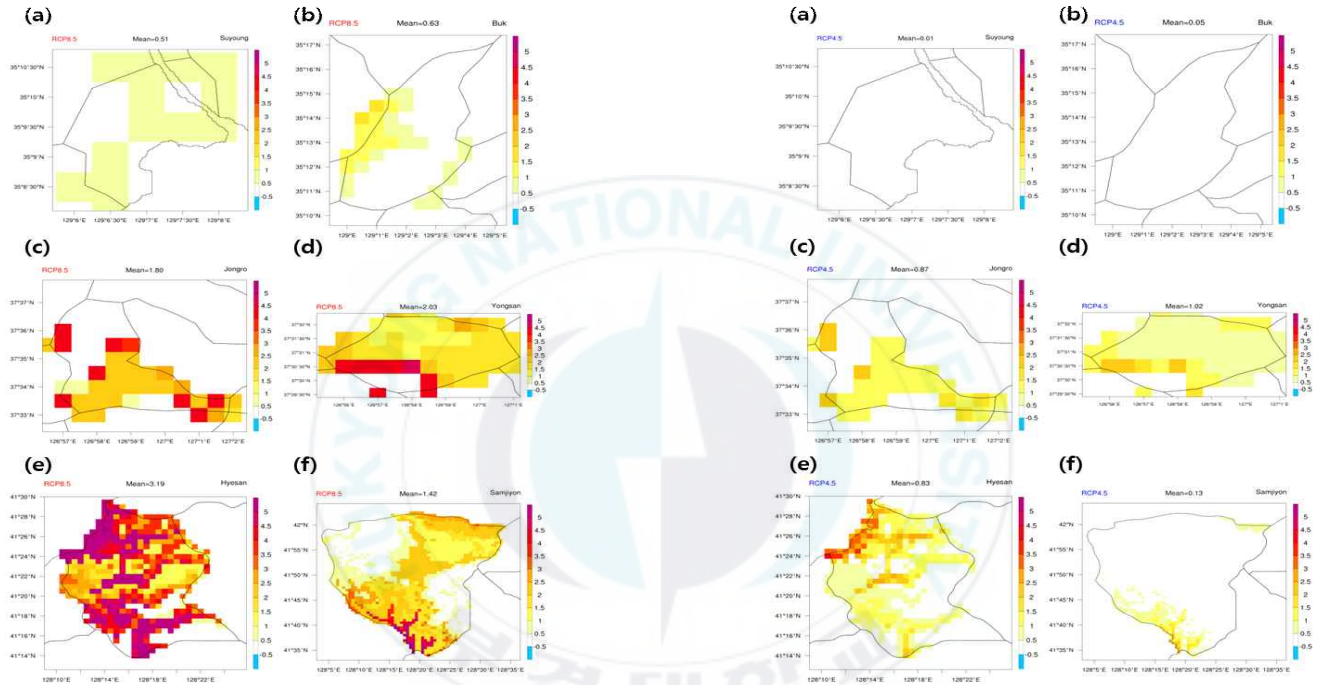


Fig. 25 Detailed regional heat wave prediction for the far-future climate based on the RCP 8.5 scenario over Korean Peninsula

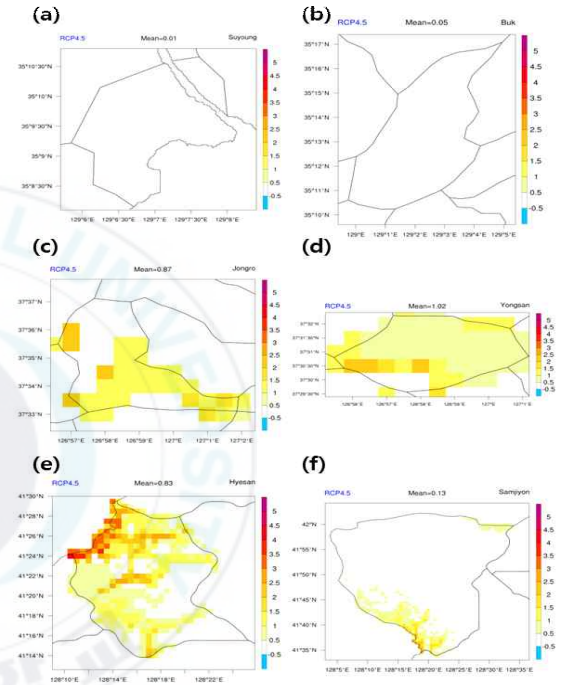


Fig. 26 Detailed regional heat wave prediction for the far-future climate based on the RCP 4.5 scenario over Korean Peninsula

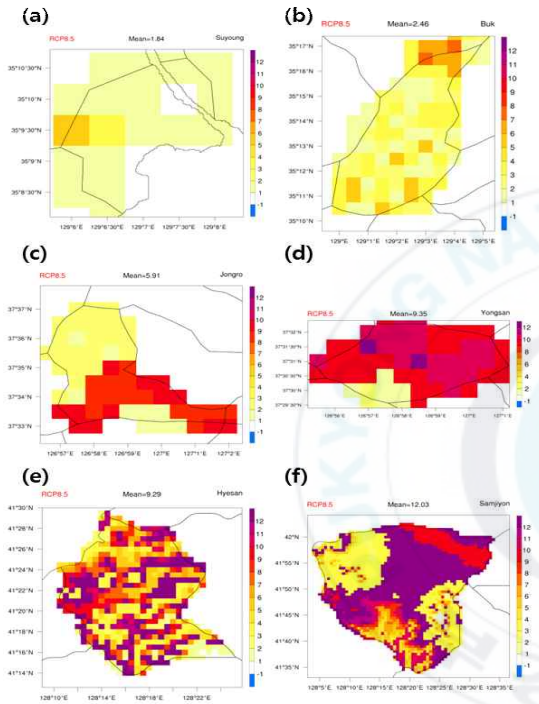


Fig. 27 Detailed regional tropical night prediction for the far-future climate based on the RCP 8.5 scenario over Korean Peninsula

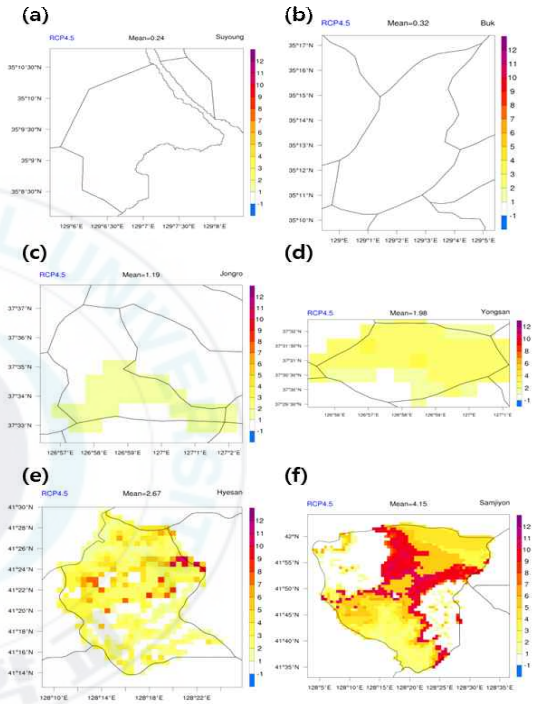


Fig. 28 Detailed regional tropical night prediction for the far-future climate based on the RCP 4.5 scenario over Korean Peninsula

V. Conclusion and Summary

In this study, we estimated 1 km of detailed precipitation / temperature over Korean Peninsula through QPM / QTM based on global climate model GME data of 40 km resolution according to RCP scenarios. This is considered physics process that is not represented by a statistical downscaling model.

In order to produce future climate prediction data based on the observed data, we restored the 1 km resolution precipitation / temperature data of the whole region of Korean Peninsula through QPM / QTM based on the observation data of the present climate (2000-2014). The accuracy of restoration through QPM / QTM was verified through the verification process using restored precipitation / temperature data. Finally, we produced future climate projections based on observation data using the model bias between the precipitation / temperature data based on observations during the present climate (2000-2014) and the precipitation / temperature data based on the GME model results.

As a result of the verification of the restored precipitation in South Korea, the hit rate of restoration was considerably high. The POD, which represents the accuracy ratio of the restored precipitation to the actual precipitation, was high and the FAR was low in all cases. The result of the verification of the restored precipitation in North Korea shows that the restoration accuracy is relatively low in all cases than the case in South Korea. And also, as a result of the verification of the restored temperature, the restored temperature tends to be slightly

underestimated to the actual temperature with respect to the verification points. In particular, the higher the altitude, the greater the temperature change due to the topographic effect.

Using the 1 km future precipitation / temperature prediction data, we analyzed the changes of climate change and extreme events in local governments which were limited by the result of the future climate based on the global climate model. In the case of extreme events related to precipitation over all regions of Korean Peninsula according to the RCP scenarios, it is expected the event is higher in Buk than Suyoung in Busan, is higher in Jongro than Yongsan in Seoul, is higher in Samjiyon than Hyesan in Yanggang. In case of extreme events related to temperature, it is predicted that increase of extreme events will be relatively high in Buk (Busan), in Yongsan (Seoul), in Samjiyon (Yanggang) in all scenarios. Overall, in all scenarios, the increase of precipitation related extreme events was expected to be large and the increase of temperature related extreme events was predicted to be small in regions with higher average latitude.

Using the 1 km future climate prediction data over Korean Peninsula produced through this study, it is possible to analyze detailed regional future climate changes.

In addition, the analysis data of future climate change and extreme events of 1 km resolution of precipitation / temperature over Korean Peninsula can be used as basic data of scientific basis in preparing responses in various application fields.

VI. Reference

- 국립 환경과학원, 2010: 한국 기후변화 평가보고서, 환경부.
- IPCC 제 5차 평가보고서(2013. 9. IPCC AR5 WG I).
- 김맹기, 한명수, 장동호, 백승균, 이우섭, 김연희, 김성, 2012: 1km 해상도의 관측 격자자료 생산기술, 기후연구 **7**(1), 55-68.
- 변재영, 이선용, 손승희, 2000: ARPS 모델을 이용한 한반도 강수량 예보 결과의 검증. 한국기상학회지 **36**(3), 337-352.
- 안중배, 허지나, 심교문, 2010: 수치예보모형을 이용한 역학적 규모 축소 기법을 통한 농업기후지수 모사. 한국농림기상학회지 **12**(1), 1-10.
- 김맹기, 김선애, 김연희, 2013: 다중 RCM 자료와 PRIDE 모델에 기반한 고해상도 남한 기후변화 전망. 한국기후변화학회 하반기 학술대회, 123.
- 배효준, 2015: 강수진단모형을 이용한 미관측 지역 상세 강수량 자료 복원 방법에 관한 연구. 부경대학교 학위논문(석사).
- 차주완, 석미경, 박종서, 2012: 기상청 기상레이더강수량추정기술 현황 및 계획. 한국수자원학회지 **45**(8), 50-55.
- 이정순, 이용희, 하종철, 이희춘, 2012: 지형을 고려한 기온 객관분석 기법. *Korean Meteorological Society*, **2**, 233-243.
- 이경미, 성장형, 김영오, 이승호, 2011: 한국에서 평균기온 및 극한기온 변화시점 분석. 대한지리학회지 **46**(5), 583-596.
- 이승호, 허인혜, 이경미, 권원태, 2005: 우리나라 상세기후지역의 구분. 한국기상학회지 **41**(6), 983-995.
- 박창용, 최영은, 권영아, 권재일, 이한수, 2013: 남한 상세 기후변화 시나리오를 이용한 아열대 기후대 및 극한기온사상의 변화에 대한 연구. 한국지역지리학회지 **19**(4), 600-614.
- 박창용, 최영은, 문자연, 윤원태, 2009: 기온과 강수특성을 고려한 남한의 기후 지역구분. 대한지리학회지 **44**(1), 1-16.
- Mao, Q., S. F. Mueller and H. H. Juang, 2000: Quantitative precipitation forecasting for Tennessee and Cumberland river watersheds using the NCEP regional spectral model. *Wea. Forecasting*, **15**, 29-45.
- Ahn, J. B., C. K. Park and E. S. Im, 2002: Reproduction of regional scale surface air temperature by estimating systematic bias of mesoscale numerical model. *J. Kor. Meteor. Soc.*, **38**, 69-80.

- Barnes, S. L., 1964: A technique for maximizing details in numerical weather map analysis. *J. Appl. Meteor.*, **3**, 396-409.
- Barnes, S. L., 1973: Mesoscale objective map analysis using weighted time-series observations., NOAA Tech. Memo. ERL NSSL-62, National Severe Storms Laboratory, Norman, OK 73069.
- Choi, Y., 2002: Trends in daily precipitation events and their extreme in the southern region of Korea. *Korea Soc. Environmental Impact Assessment*, **11**, 189-203.
- Collier, C. G., 1975: A representation of the effects of topography on surface rainfall within moving baroclinic disturbances. *Q. J. R. Meteor. Soc.*, **101**, 407-422.
- Daly, C., Neilson, R. P., and Phillips, D. L., 1994: A statistical-Topographic Model for Mapping Climatological Precipitation over Mountainous Terrain, *Journal of Applied Meteorology and Climatology*, **33**, 140-158.
- Haylock, M., and N. Nicholls, 2000: Trends in extreme rainfall indices for an updated high quality data set for Australia, 1910-1998. *Int. J. Climatol.*, **20**, 1533-1541.
- Kim, Ok-Yeon and Jai-Ho Oh, 2010: Verification of the Performance of the High Resolution QPF Model for Heavy Rainfall Event over the Korean Peninsula, *Asia-Pacific Journal of Atmospheric Sciences*, **46**(2), 119-133.
- Misumi, R., V. A. Bell and R. J. Moore, 2001: River flow forecasting using a rainfall disaggregation model incorporating small-scale topographic effects. *Meteor. Appl.*, **8**, 297-305.
- Sinclair, M. R., 1994: A diagnostic model for estimating orographic precipitation. *Journal of Applied Meteorology*, **33**, 1164-1175.
- McBride, J. L., E. E. Ebert, 2000: verification of quantitative precipitation forecasts from operational numerical weather prediction models over australia. *Wea. Forecasting*, **15**, 103-121.
- E. S. Im, M. H. Kim, W. T. Kwon, 2007: Projected Change in Mean and Extreme Climate over Korea from a Double-Nested Regional Climate Model Simulation. *Journal of Meteorological Society of Japan*, **85**(6), 717-732.

- Y. Hundecha, A. Bardossy, 2008: Statistical downscaling of extremes of daily precipitation and temperature and construction of their future scenarios, *Int. J. Climatol.*, **28**, 589–610.
- J. Li, Z. Wu, Z. Jiang, J. He, 2010: Can Global Warming Strengthen the East Asian Summer Monsoon?. *J. Climate*, **23**, 6696–6705.
- J. Y. Hong, J. B. Ahn, 2015: Changes of Early Summer Precipitation in the Korean Peninsula and Nearby Regions Based on RCP Simulations. *J. Climate*, **28**, 3557–3578.

